

University of Windsor

Scholarship at UWindor

Electronic Theses and Dissertations

Theses, Dissertations, and Major Papers

1-1-1970

Electrical conductivity characteristics and phase relationships in vanadium oxide-boric oxide system.

T. K. Vaidyanathan
University of Windsor

Follow this and additional works at: <https://scholar.uwindsor.ca/etd>

Recommended Citation

Vaidyanathan, T. K., "Electrical conductivity characteristics and phase relationships in vanadium oxide-boric oxide system." (1970). *Electronic Theses and Dissertations*. 6876.
<https://scholar.uwindsor.ca/etd/6876>

This online database contains the full-text of PhD dissertations and Masters' theses of University of Windsor students from 1954 forward. These documents are made available for personal study and research purposes only, in accordance with the Canadian Copyright Act and the Creative Commons license—CC BY-NC-ND (Attribution, Non-Commercial, No Derivative Works). Under this license, works must always be attributed to the copyright holder (original author), cannot be used for any commercial purposes, and may not be altered. Any other use would require the permission of the copyright holder. Students may inquire about withdrawing their dissertation and/or thesis from this database. For additional inquiries, please contact the repository administrator via email (scholarship@uwindsor.ca) or by telephone at 519-253-3000ext. 3208.

ELECTRICAL CONDUCTIVITY CHARACTERISTICS

AND PHASE RELATIONSHIPS

IN $V_2O_5 - B_2O_3$ SYSTEM

By

T. K. VAIDYANATHAN

A THESIS

Submitted to the Faculty of Graduate Studies
Through the Department of Engineering Materials

In Partial Fulfillment of the Requirements

for the degree of

MASTER OF APPLIED SCIENCE

at the University of Windsor

WINDSOR, ONTARIO

1 9 7 0

UMI Number: EC52841

INFORMATION TO USERS

The quality of this reproduction is dependent upon the quality of the copy submitted. Broken or indistinct print, colored or poor quality illustrations and photographs, print bleed-through, substandard margins, and improper alignment can adversely affect reproduction.

In the unlikely event that the author did not send a complete manuscript and there are missing pages, these will be noted. Also, if unauthorized copyright material had to be removed, a note will indicate the deletion.

UMI[®]

UMI Microform EC52841

Copyright 2008 by ProQuest LLC.

All rights reserved. This microform edition is protected against unauthorized copying under Title 17, United States Code.

ProQuest LLC
789 E. Eisenhower Parkway
PO Box 1346
Ann Arbor, MI 48106-1346

ABM8539

ABSTRACT

Electrical conductivity studies were carried out in the system $B_2O_3 - V_2O_5$ with small additions of sodium oxide having a fixed mole fraction ratio of 0.01 Na_2O to 0.99 B_2O_3 to determine, at constant temperature, the variation with vanadia content of the specific and molar conductivities.

The present work indicates that the conductivity variation is not a direct function of the vanadia content but is rather a function of the solubility of vanadia in the B_2O_3 containing 1 mole % Na_2O , the nature of the vanadium ion as well as a heretofore undetermined liquid miscibility gap in the $V_2O_5 - B_2O_3$ system.

¹
299072

APPROVED BY

AB .5C

J. Rees

C. P. Lane

ACKNOWLEDGEMENTS

I wish to gratefully acknowledge the guidance, encouragement and criticism of Professor Billinghamurst throughout this work.

The financial support for this project was provided by the National Research Council of Canada.

CONTENTS

	Page
ABSTRACT	i
ACKNOWLEDGEMENTS	iii
TABLE OF CONTENTS	iv
LIST OF FIGURES	vi
LIST OF TABLES	vii
I. INTRODUCTION	1
II. LITERATURE REVIEW	2
III. EXPERIMENTAL	
A. Initial problems	12
B. Apparatus used	12
C. Cell arrangement	13
D. Cell constant determination	13
E. Temperature measurement	15
F. Temperature compensation for cell constant	18
G. Resistance of leads and electrodes	18
H. Determination of density of melt	18
I. General experimental procedure	19
J. Cooling curves.	21
IV. RESULTS	
A. Electrical conductivity	24
B. Phase diagram modifications	24
C. Agreement with previous results	25

	Page
V. DISCUSSION OF RESULTS	26
A. Variations of specific conductivity with mole % V_2O_5	27
B. Variation of molar conductivity with mole % V_2O_5	30
C. Electrical conductivity and phase separation	30
D. Visual examination	33
E. Monotectic temperature	33
F. Examination of immiscibility	36
G. Variation of E_k with mole % V_2O_5 and the conductivity changes from 0 to 100 mole % V_2O_5	37
VI. CONCLUSIONS	43
VII. REFERENCES	45
VIII. APPENDIX I	48
Electrical conductivity data and calculations	
IX. APPENDIX II	
Activation energy plots	66
X. APPENDIX III	
Nomenclature	81
XI. VITA AUCTORIS	82

FIGURES

	Page
1. General experimental set-up	14
2. Relationship of liquid height vs. cell constant	17
3. Relationship of liquid height vs. volume in crucible	21
4. Relationship of $\log_{10} K$ vs. mole % V_2O_5	29
5. Relationship of $\log_{10} \Lambda_M$ vs. mole % V_2O_5 .	32
6. Cooling curves at monotectic composition region	34
7. A. Phase diagram of $B_2O_3 - V_2O_5$ system	35
B. Modified phase diagram	
8. Activation energy of conductance E_k vs. Mole % V_2O_5	39
9. Plot of $\log_{10} K$ vs. $\frac{1}{T}$ for sample 1	67
10. Plot of $\log_{10} K$ vs. $\frac{1}{T}$ for sample 2	68
11. Plot of $\log_{10} K$ vs. $\frac{1}{T}$ for sample 3	69
12. Plot of $\log_{10} K$ vs. $\frac{1}{T}$ for sample 4	70
13. Plot of $\log_{10} K$ vs. $\frac{1}{T}$ for sample 5	71
14. Plot of $\log_{10} K$ vs. $\frac{1}{T}$ for sample 6	72
15. Plot of $\log_{10} K$ vs. $\frac{1}{T}$ for sample 7	73
16. Plot of $\log_{10} K$ vs. $\frac{1}{T}$ for sample 8	74
17. Plot of $\log_{10} K$ vs. $\frac{1}{T}$ for sample 9	75
18. Plot of $\log_{10} K$ vs. $\frac{1}{T}$ for sample 10	76
19. Plot of $\log_{10} K$ vs. $\frac{1}{T}$ for sample 11	77
20. Plot of $\log_{10} K$ vs. $\frac{1}{T}$ for sample 12	78
21. Plot of $\log_{10} K$ vs. $\frac{1}{T}$ for sample 13	79
22. Plot of $\log_{10} K$ vs. $\frac{1}{T}$ for sample 14	80

TABLES

	Page
1. Cell constants	16
2. Height and volume in Pt crucible at room temperature	20
3. Mole % V_2O_5 and $\log_{10} K$ at 700°C and 800°C.	28
4. Mole % V_2O_5 and $\log_{10} \Lambda_M$ at 700°C and 800°C	31
5. Mole % V_2O_5 and E_k values	38
6. Conductivity data and calculations for sample 1	49
7. Conductivity data and calculations for sample 2	50
8. Conductivity data and calculations for sample 3	51
9. Conductivity data and calculations for sample 4	52
10. Conductivity data and calculations for sample 5	53
11. Conductivity data and calculations for sample 6	54
12. Conductivity data and calculations for sample 7	55
13. Conductivity data and calculations for sample 8	56
14. Conductivity data and calculations for sample 9	57
15. Conductivity data and calculations for sample 10	58
16. Conductivity data and calculations for sample 11	59
17. Conductivity data and calculations for sample 12	60
18. Conductivity data and calculations for sample 13	61
19. Conductivity data and calculations for sample 14	62
20. $\log_{10} K$ vs. $\frac{1}{T}$ data.	63

INTRODUCTION

Electrical conductivity studies have been used in the past to reveal structural features of borate melts. Many investigations of systems involving boric oxide have been conducted without conclusively revealing a basic structural model for liquid boric oxide and borates.

Vanadium pentoxide is the other major component involved in the system under the present investigation. This is another glass former in conjunction with certain oxides although vanadium pentoxide does not by itself form glass on solidification. The nature of the liquid melt is also not well established in the case of V_2O_5 .

There is practical interest in the study of electrical conductivity and phase relationships in the system $B_2O_3 - V_2O_5$. Thus, the electrical conductivity data of borate oxide systems are of interest in exploring the potential electrolysis of such borate melts.

The object of the present investigation was therefore to obtain such electrical conductivity data and to correlate the variation of electrical conductivity with the composition, the phase relationships and the bonding characteristics of the melt in different composition regions.

LITERATURE REVIEW

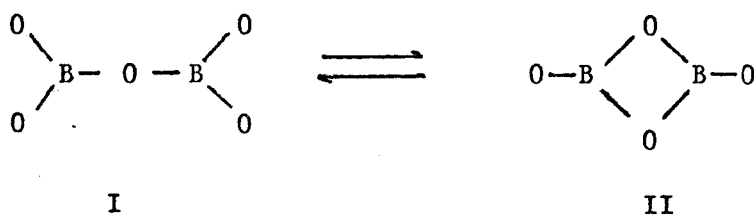
The first recorded study of electrical conductivity of boron trioxide was that of Tichanowitsch (1). It was reported as a non-conductor, obviously due to the limitations of the conductivity bridge used.

The electrical conductivity of boron trioxide was studied by Arndt and Gessler (2). The specific conductivity was reported to vary from $7 \times 10^{-6} \text{ ohm}^{-1} \text{ cm}^{-1}$ at 800°C to $46 \times 10^{-6} \text{ ohm}^{-1} \text{ cm}^{-1}$ at 1000°C .

In a detailed investigation on the electrical conductivities of alkali borates, Shartsis et al (3) observed the sharp increase in the electrical conductivity of boric oxide for the first additions of alkali oxide. The specific conductivity of liquid alkali borates containing 1 mole per cent of metal oxide is approximately ten times greater than that of pure boric oxide. The temperature coefficient of conductance is positive. The magnitude of the specific conductivity and the energy of activation of conductance are of the same order as that of silicates. The alkali borates are therefore classified as ionic liquids. The experimental observations on density, increase of activation energy for viscous flow and the electrical conductivity studies indicate that the "network-breaking" effect due to metal oxide is not the only predominant mechanism in altering the

structure of boric oxide. An equilibrium between BO_3 triangles and BO_4 tetrahedra is suggested to exist in the melt. Increasing the metal oxide content and increasing the temperature favour the latter configuration.

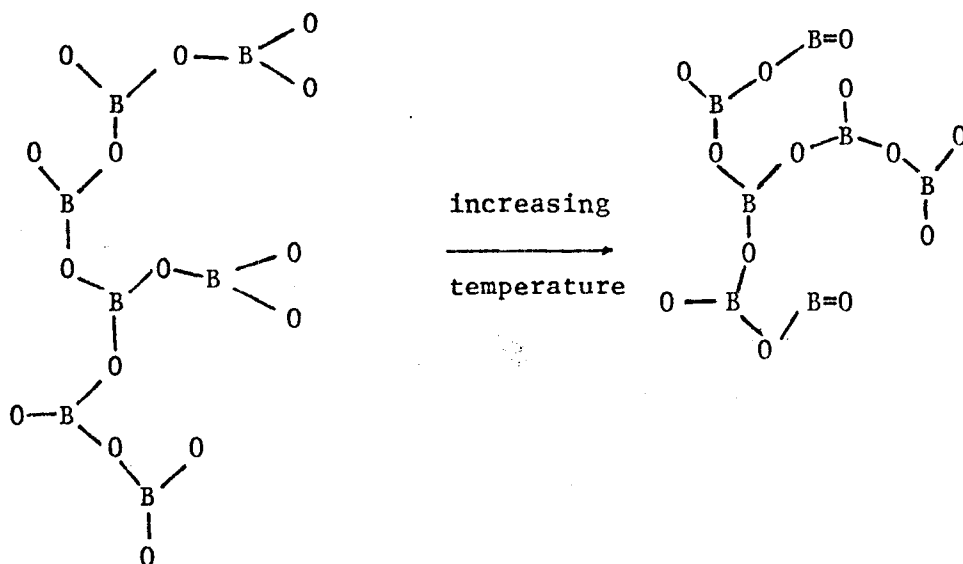
Studies on viscosity, density and electrical conductivity of liquid boric oxide by Mackenzie (4) indicated that the structure of liquid B_2O_3 is temperature dependent. Ionic dissociation is negligible even up to temperatures as high as 1000°C . The results were explained on the basis of a model of one boron atom being bonded to two oxygen atoms as postulated in (5). The liquid boric oxide has the following equilibrium structures:



By increasing the temperature, structure II is favoured. This suggestion however necessitates a smaller $-\text{B}-\text{O}-\text{B}$ angle and therefore a closer packing and a higher density. On increasing the temperature, the density of liquid boric oxide is expected to show a positive deviation from linearity. The molar volume vs. temperature curve shows a tendency to corroborate this (6).

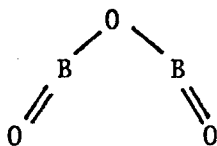
An extensive x-ray diffraction study by Zarzeki (7) indicated that the coordination of oxygen around boron changes with temperature and has the value of 3.3, 2.3 and 2.2 at 20°C, 1200°C and 1600°C respectively. This was attributed to increasing ionic dissociation of the boric oxide with rise in temperature giving rise to free O^{--} ions. At 1200°C, 30% B-O bonds are ruptured. The concentration of free O^{--} ions in the melt is thus 15%.

Mackenzie (8) studied the electrical conductivity of boric oxide at elevated temperatures to explore the possibility of ionic dissociation in the melt at elevated temperatures. The electrical conductivity remains low at high temperatures indicating that no dissociation of the melt takes place. A model of the liquid boric oxide structure was proposed to account for the viscosity, density and electrical conductivity data.



The structure of boric oxide in the vapour state suggested by

White et al (9)

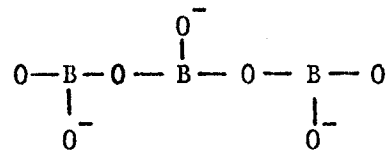


supports the above model. The infrared emission maximum observed at 2041 cm^{-1} was attributed to the B = O stretchings. Negative departure from linearity in molar volume is explained by the shorter B = O bondings. Decreasing association in the liquid is evident as some parts of the continuous network are terminated at every B = O. Preliminary examination of infrared spectra of glassy B_2O_3 chilled from 1000°C has indeed revealed the presence of a maximum of about 2050 cm^{-1} . Confirmation of this hypothesis however needs further work.

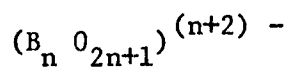
The electrical conductivity characteristics of the system $\text{PbO-B}_2\text{O}_3$ were investigated in detail by Bockris and Mellors (10) over the whole range of compositions. They also made subsidiary measurements on the density of the system. The equivalent conductivity increases with mole per cent of PbO. The variation of activation energy with mole per cent PbO shows characteristic increase and decrease which were explained on the basis of satisfactory models. They also considered that pure liquid boric oxide has an appreciable intrinsic conductance.

On the basis of the variations, the following structural models were postulated analogous to silicates:

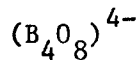
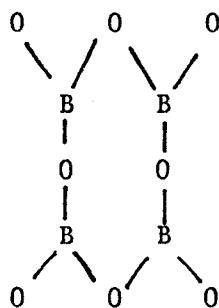
- 1) Above 75 mole per cent PbO, the planar discrete BO_3 ion is the sole anionic constituent of the melt.
- 2) As B_2O_3 is increased above 25 mole per cent, the formation of the chain begins as follows:



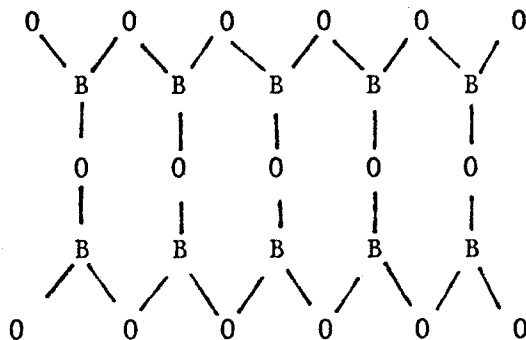
The formula for such a chain is:



- 3) When $\frac{\text{O}}{\text{B}} = 2$, the chains rapidly increase to a very great length. Near to the composition 50 mole % PbO, the rapid increase in length of the chain makes it unstable and causes break down to form rings. Among the several possible ring systems, they suggested the model based on the four boron atom rings



growing to chain rings of the type



up to about

$(B_{40} O_{60})^{6-}$ an ion containing about 20 rings at 8 mole % PbO, where a sharp inflection in molar volume occurs. The -B-O-B angle in such a ring would be 135° whereas the observed angle is about 150° .

- 4) It was also suggested that PbO may act as a bridging central atom at the high PbO contents.
- 5) A rapid decrease of heat of activation for conductance occurs during addition of the first 8 mole % of PbO. It was proposed that the B-O-B bonds are broken and the Pb^{++} is presented with a rapidly increasing ease of passage from one interstice to the next. The tendency is complete at 8 mole % PbO when discrete borate ions begin formation.

While the existence of such discrete anions in the melt is essentially possible, the increasing anionic sizes with increasing boric oxide is not compatible with the

observed viscosity data (11). The model also entirely ignores the possibility that BO_4 tetrahedra can become the more important configuration in certain borate glasses (12).

Another model for liquid boric oxide had earlier been proposed by Fajans and Barber (13). Liquid boric oxide is considered as a molecular liquid consisting of B_4O_6 molecules. Anderson et al (14) proposed that liquid boric oxide is an ionic melt involving complex boron-oxygen ions. Liquid boric oxide was also considered as a highly associated network of interlinking BO_3 triangles by Warren et al (15).

It is thus clear that the extensive experimental investigations carried out in borate and boric oxide melts have not yet revealed a basic structural model which can explain the various observations in these melts. The application of any structural model for borate melts is not as simple as for silicates.

Noting this difference between silicates and borates, Weyl and Marboe (16) postulated that liquid boric oxide is closely related to organic polymers and not related to the stable form of liquid SiO_2 . The liquid boric oxide is considered as a Stewart type liquid. Stewart (17) had earlier proposed that molecular liquids may contain swarms

of molecules which show some degree of temporary order. Thus the idea of time as a parameter in the structure of liquid boric oxide was also introduced.

The crystal structure of boric oxide B_2O_3 was determined as hexagonal by Berger (18) based on powder diffraction data. This form of B_2O_3 is now known to be $(B_2O_3)_{15}H$ (20). Senkovitz and Hawley (21) reported the crystalline form of pure B_2O_3 as cubic.

The electrical conductivity of vanadium pentoxide was first studied by Buff (22). He observed that it had good conductivity. Van Arkel et al (23) studied the electrical conductivities of some oxides including vanadium pentoxide. The general temperature dependence of electrical conductivity was evaluated in the linear form $\log K = A + \frac{B}{T}$ and in the quadratic form $\log K = A + \frac{B}{T} + \frac{C}{T^2}$. The values of A and B in the linear relationship $\log K = A + \frac{B}{T}$ were reported as $A = 4.670$ and $B = -6.427$ respectively. The relationship $\log K = A + \frac{B}{T} + \frac{C}{T^2}$ gave the values of A, B and C as -26.368 , 67313 and -43.767×10^{-6} respectively. The extrapolated value of specific conductance K at melting point was evaluated as $0.00999 \text{ ohm}^{-1} \text{ cm}^{-1}$ in the linear plot and as $0.000217 \text{ ohm}^{-1} \text{ cm}^{-1}$ in the quadratic relationship.

The corresponding equivalent conductance values were given as $0.107 \text{ ohm}^{-1} \text{ moles}^{-1} \text{ cm}^{-1}$ and $-.00235 \text{ ohm}^{-1} \text{ moles}^{-1} \text{ cm}^{-1}$ in the linear and quadratic forms.

The activation energy of conductance gave a value of $E_k = 29.4 \text{ k cal/mole}$ in the linear relationship whereas in the quadratic plot, the values of E_k at different temperatures gave the following values:

$$E_k \text{ at M P} = 107.9 \text{ k cal/mole}$$

$$E_k \text{ at } 915.5^\circ\text{C} = 33.4 \text{ k cal/mole}$$

$$E_k \text{ at } 964^\circ\text{C} = 19.5 \text{ k cal/mole}$$

A quartz capillary conductivity cell, heated by a bath of molten sodium chloride, was used. A Pt, Pt/Rh thermocouple was used for measuring the temperatures. The resistance of the cell was measured in a simple a-c bridge circuit at a frequency of 1000c/s.

The crystalline form of V_2O_5 was reported as orthorhombic (24). It is now known that this form is actually $(V_2O_5)_{140}$ (25).

Examining the nature of the liquid melts, Mackenzie (26) suggests that liquid vanadium pentoxide is probably a network type. He bases his suggestion on the extrapolated specific conductivity value at the M.P. on the quadratic plot as indicated previously.

The phase diagram for the system $B_2O_3 - V_2O_5$ was studied

by Nador (27). On the basis of investigations on five selected compositions up to and above 55 wt% of vanadium pentoxide, the liquidus curve was drawn. The X-ray analysis indicated no compound formations.

Levin (28) mentions that vanadium ion is five coordinated with oxygen, so that four oxygen atoms lie in one plane whereas the fifth oxygen lies perpendicular to this plane, with an exceptionally short V-O distance.

Vanadium has also been reported in octahedral coordinations in KV_3O_8 and CsV_3O_8 (29) and in tetrahedral coordination in $NaVO_3$ and KVO_3 (30).

EXPERIMENTAL

A. Initial Problems

One of the major problems in studying the boric oxide systems is the very corrosive nature of the molten boric oxide. Initially attempts were made to use "Coors" recrystallized alumina crucibles, but these crucibles cracked during the cooling cycles of the trial experiments. Therefore, platinum crucibles were selected to avoid this problem. Platinum had been used in the past for similar studies on boric oxide systems.

The second major problem is the foaming of the moisture content of the boric oxide in the mixtures. Careful trial experiments were made to standardize a heating cycle to avoid this foaming. The foaming was eliminated by holding the mixture at 600°C for 4 hours before heating the mixture to the required temperature.

B. Apparatus Used

A crucible furnace capable of giving as high a temperature as 1300°C was used throughout the investigation.

Temperature control was achieved by means of a regulator which controlled the power input corresponding to a set efficiency percentage. By setting the regulator knob at any given per cent efficiency, it is possible to maintain a required temperature at the crucible zone. An initial standardization of the furnace temperatures vs. regulator setting provided a very reliable chart for temperature control by regulator knob setting.

By introducing a thick alumina tube between the open winding of the resistance element and the material to be heated, the temperature within the shield was held to reproducible values of $\pm 2^{\circ}\text{C}$ at the crucible zone.

A Leeds and Northrup Electrolytic Conductivity Bridge 4959 was used for the electrolytic conductivity measurement. It operates on two frequencies, 50c/s and 1000c/s.

C. Cell Arrangement

The arrangement was similar to some degree with that of Bockris and Mellors (10). Platinum electrodes (2mm dia.) and a platinum crucible (capacity of crucible = 50ml) were used in the experiments.

The electrodes were rigidly inserted into alumina tubes with a matching bore, reinforced with tight fitting outer alumina tubes with a matching bore and the tubes in turn were fitted through drilled holes 2 cm. apart in a thick asbestos plate. The thermocouple was inserted through another drilled hole on the asbestos plate. The alumina tubes carrying the platinum electrodes were then rigidly cemented to the asbestos plate, such that when placed over the furnace covered with another asbestos plate having a central hole to accommodate the assembly, the electrodes projected into the crucible to about 1" when the crucible was placed at the center of the furnace chamber. The crucible itself was positioned at the center of the furnace chamber within the alumina tube on a hole in a shaped brick placed at the bottom of the furnace chamber. During the cell constant determinations, reproducibility was found to be $\pm 1\%$.

The overall arrangement is shown in figure 1.

D. Cell Constant Determination

The cell constant was determined for different depths of the liquid

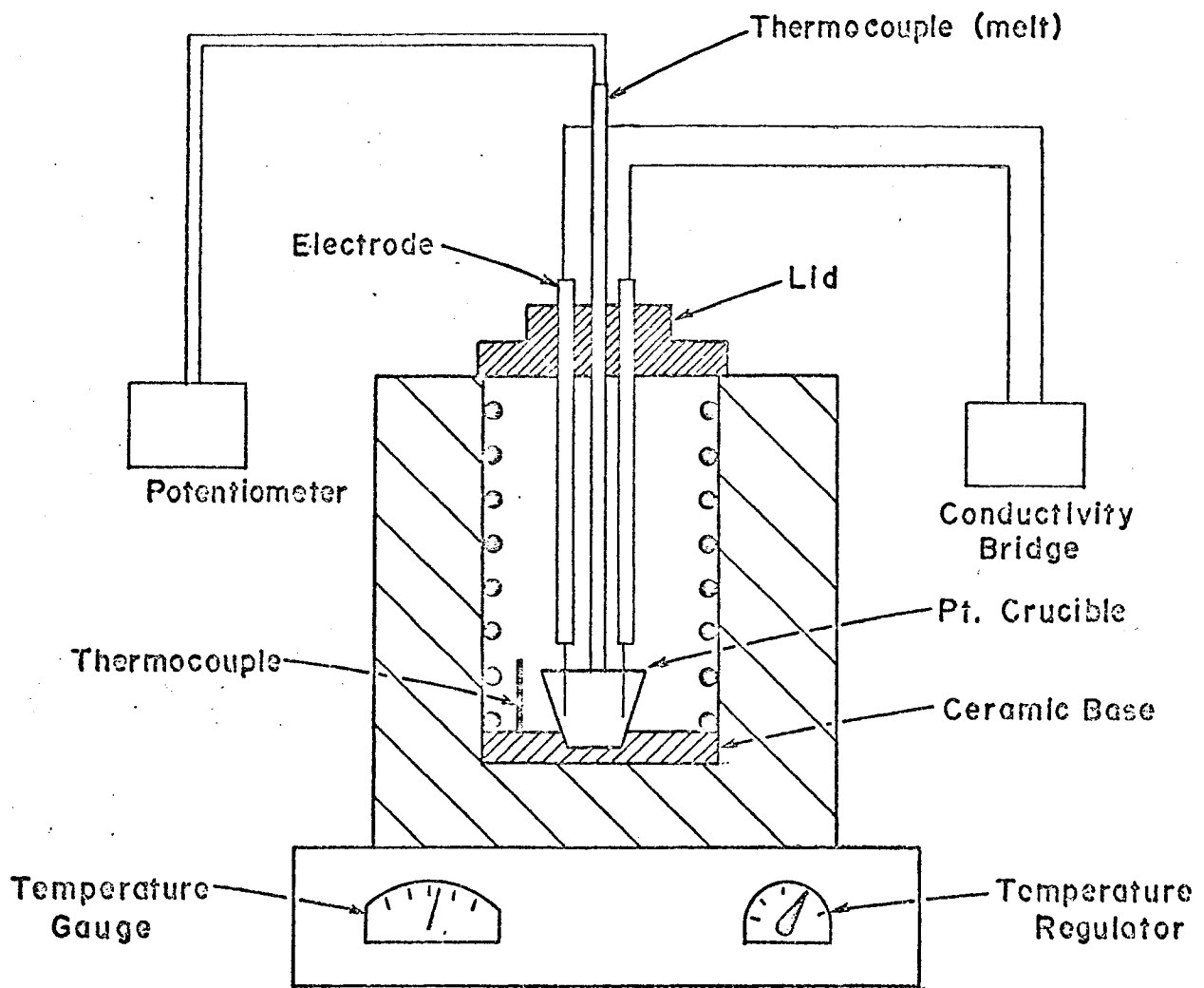


FIG. 1 GENERAL EXPERIMENTAL
SET-UP

in the crucible. Here 0.1 N KCl solutions were used for the cell constant determination and the results are summarized in Table 1. The electrodes were platinized by immersing them in a solution containing 0.02 gm. lead acetate and 3 gm. platinum chloride in 100 cc. of distilled water and connecting them to two dry cells connected in series. A rheostat was used to control the gas evolved. The electrodes were then washed thoroughly with distilled water. All traces of chlorine adsorbed from the plating solution were removed by the usual procedure of continuing the electrolysis with the same connections in a dilute solution of sulphuric acid. The conductivity of the distilled water used was of the order of 10^{-6} ohm⁻¹ cm⁻¹ and no correction was made for this value. Reagent grade KCl was used for the standard solutions.

A plot of cell constant vs height of solution in the crucible yielded a smooth curve. Fig. 2 shows the curve and appears to follow the trend of the similar curve obtained by Bockris and Mellors (10).

E. Temperature Measurement

A Pt - Pt, Rh thermocouple with the bottom end covered with Pt foil over an alumina sheath carrying the thermocouple wires was used to measure the temperature of the melt during initial standardization. For each composition, the temperature of the melt was standardized against a chromel-alumel thermocouple outside the melt. The electrical conductivity was measured without introducing any fluctuations in the cell constant by inserting the thermocouple in the melt when the electrical conductivity was measured. The chromel-alumel thermocouple was replaced after every third run.

TABLE 1
CELL CONSTANT DETERMINATION

0. 1 N KCl Solution

Temp. 25°C

Platinized Electrodes

Specific Conductivity of

0. 1 N KCl Solution = K^{KCl} at 25°C = 12856.0 micro mhos
0. 1 N

H Height of KCl Solution Divisions (1 Div. = 0.2")	G_M Measured Conductance ohms ⁻¹	K Cell Constant cm ⁻¹ $\frac{GM}{K^{KCl}} = \frac{GM}{1.2856 \times 10^{-2}}$ 0. 1 N
4.7	1.09×10^{-2}	0.8479
5.1	1.195×10^{-2}	0.9300
5.4	1.26×10^{-2}	0.9800
6.2	1.36×10^{-2}	1.058
6.7	1.49×10^{-2}	1.159
7.2	1.52×10^{-2}	1.182
7.5	1.530×10^{-2}	1.190

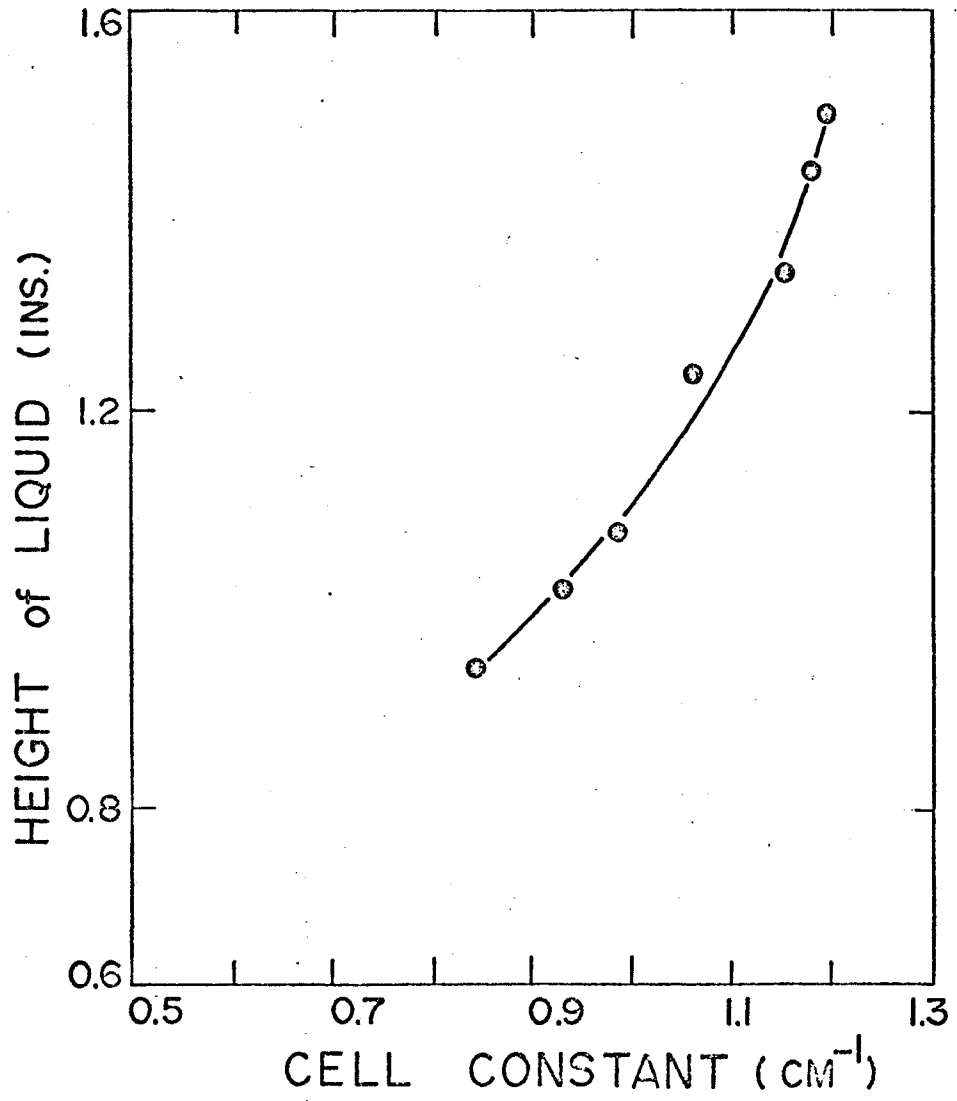


FIG. 2 RELATIONSHIP OF LIQUID HEIGHT VS. CELL CONSTANT

F. Temperature Compensation For Cell Constant

The liquid heights in the crucible were measured at 750°C. The corresponding cell constants were read off from the cell constant vs. liquid height chart. As the correction for a temperature variation of $\pm 50^\circ\text{C}$ (the temperature range studied was 700 - 800°C) was less than 1%, no further corrections for cell constant was made to account for the temperature variation.

G. Resistance of Leads and Electrodes

The resistance of leads and electrodes was determined by joining the electrode ends by a platinum rod. The resistance varied between $5 \times 10^{-6} \Omega$ to $6 \times 10^{-6} \Omega$ for the temperature range of 700°C and 800°C.

H. Determination of Density of Melt

Densities were required for the molar conductivity determinations. The volumes of the melts used had to be determined for each temperature. An approximate method was used to obtain the volumes needed. The height vs. volume of liquid in the platinum crucible was initially plotted for room temperature using distilled water and experimentally determining the volume against a measured height of water in the platinum crucible. A correction was then made for the change of volume of the platinum crucible at a higher temperature using the expansivity data for platinum. The volume change was converted into a per cent volume change per °C and corrections applied at various temperatures.

As the platinum crucible contained weighed amounts of the mixture, the densities could be calculated. Table (2) and Fig. 3 give the room temperature relationship between volume and height of liquid in the platinum crucible.

I. General Experimental Procedure

The boric oxide, vanadium pentoxide and sodium tetraborate were thoroughly shaken together for 20 minutes. A sufficient quantity of the mixture was placed in the crucible so that, after the melting, a melt depth of about 3 to 4 cm. was obtained. A peephole in the asbestos plate provided a convenient check for the immersion and positioning of the electrodes in the melt.

The mixture was heated to about 1150°C and held there for several hours (overnight) to ensure the homogeneity of the melt. All measurements were made in the temperature range from 900°C to the liquidus temperature during heating and cooling.

As the fused boric oxide contained a certain amount of moisture, it was necessary to drive out all the water content by holding the mixture at 600°C for about 4 hours prior to homogenizing the melt at 1150°C overnight.

A trial experiment was conducted to ascertain the loss of weight of boric oxide and vanadium pentoxide samples and this yielded 0.3% by wt. and 0.28% by wt. as the losses of boric oxide and vanadium pentoxide (at 750°C for 4 hours) respectively.

TABLE 2

ROOM TEMPERATURE RELATIONSHIP
BETWEEN LIQUID HEIGHT vs VOLUME
IN PLATINUM CRUCIBLE

Height Division (1 Div. = 0.2")	Volume cc
7	36.378
6.4	31.827
5.8	26.024
4.9	21.431
3.9	14.940
3.1	11.084

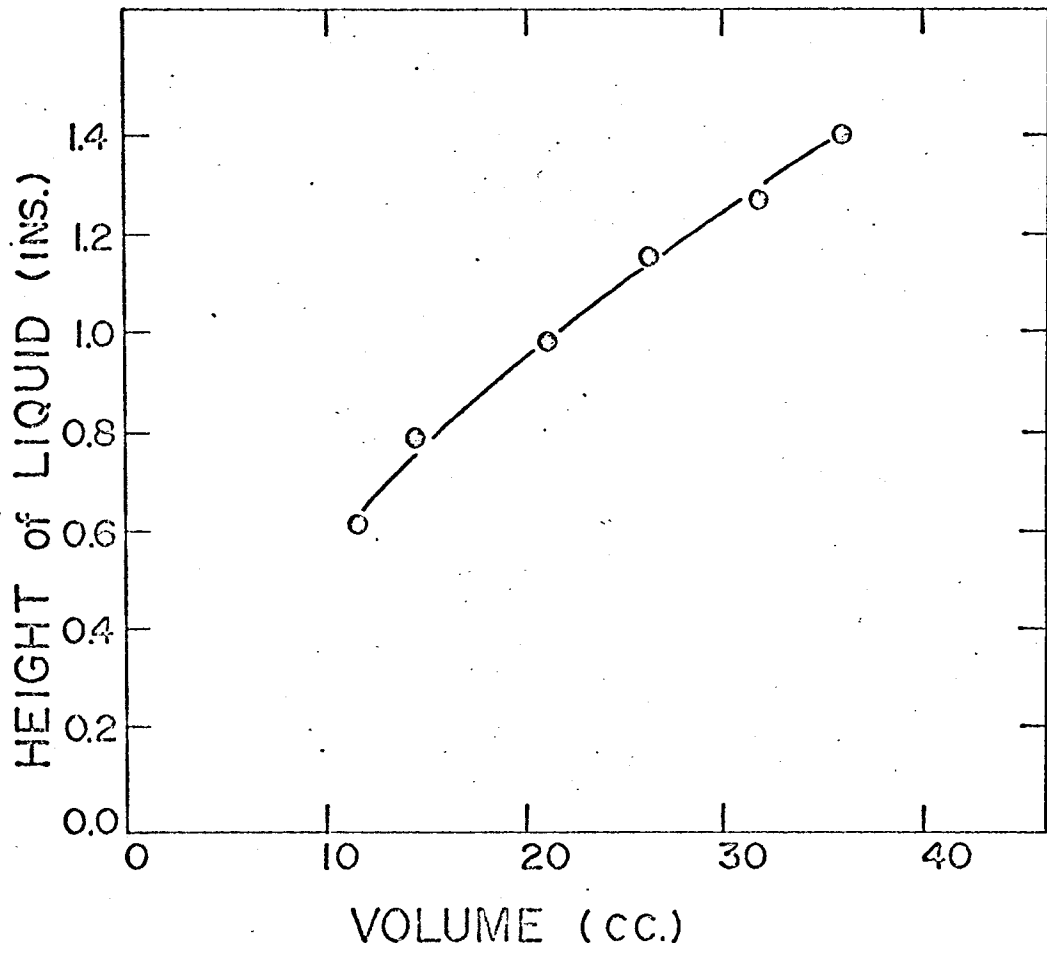


FIG. 3 RELATIONSHIP OF LIQUID HEIGHT VS. VOLUME
IN CRUCIBLE.

Trial experiments at the bridge current frequencies of 80c/s and 1000c/s to verify what Bockris and Mellors (10) and Van Arkel et al (23) reported for pure B_2O_3 and V_2O_5 respectively, confirmed that conductivity values were independent of bridge current frequency in the system $B_2O_3 - V_2O_5$ containing additions of Na_2O in the fixed mole fraction ratio of 0.99 B_2O_3 : 0.01 Na_2O . All conductivity measurements were therefore made at 1000c/s bridge current.

Electrical conductivities of mixtures of the following V_2O_5 contents were investigated:

Sample	Mole % V_2O_5
1	0
2	0.17
3	3
4	13.6
5	20
6	25
7	30
8	37
9	46.47
10	60.39
11	73
12	88
13	95
14	100

J. Cooling Curves

As indicated earlier, Nador (27) studied the system $B_2O_3 - V_2O_5$

and plotted the phase diagram on the basis of his studies on five selected compositions. The conductivities measured at high boric oxide composition region (80 to 100 mole %) indicated that his extrapolation in this region was incorrect. Visual evidence confirmed the existence of a liquid-liquid miscibility gap. Cooling curves were drawn in the liquid immiscibility composition region to ascertain the monotectic temperature and further confirm the existence of liquid immiscibility.

Samples containing 3, 5, 10, 15 and 18 mole % vanadium pentoxide were cooled from about 850 °C and the cooling curves were drawn using an automatic recorder. A chromel-alumel thermocouple with its alumina sheath covered by a platinum foil at the bottom end was used. Cooling was done outside the furnace so that a high rate of cooling was ensured and the arrest point could be readily detected.

RESULTS

A. Electrical Conductivity

The cell constant determination data are presented in Table 1 and plotted in Figure 2. Table 2 gives the room temperature relationship data between melt height and volume of melt in the crucible while Figure 3 illustrates the same graphically.

The electrical conductivity data for the samples 1 to 14 are presented in Tables 6 to 20 (Appendix I). The Tables 3 and 4 are extracted from the various electrical conductivity data in Appendix I to illustrate the isothermal variation of specific and molar conductivities respectively, with the composition of the melt. Figures 4 and 5 illustrate the corresponding relationships schematically.

The values of the activation energy of conductance in the different melt samples are obtained from the $\log_{10} K$ vs. $\frac{1}{T}$ plots in figures 9 to 22 (Appendix II). Table 5 presents the variation of activation energy values with the variation of V_2O_5 content in the melt and Figure 8 illustrates this variation schematically.

B. Phase Diagram Modifications

The cooling curves in Figure 6 indicate that the monotectic temperature in the $B_2O_3 - V_2O_5$ system is $593 \pm 5^\circ C$.

Figure 7 shows the modified phase diagram for the system $B_2O_3 - V_2O_5$ and incorporates the liquid-liquid immiscibility region established during the study.

C. Agreement with Previous Results

The results of sample 1 are in close agreement with the values of Shartsis et al (3). The activation energy of conductance of the melt (Sample 1) is 26.458 kcals/mole and is in agreement with the value obtained by Mackenzie (32).

The results for vanadium pentoxide agree closely with the linear extrapolation values of Van Arkel et al (23) at temperatures near to the melting point, but the activation energy E_k value is in disagreement up to a value of 12 k cal/mole. The quadratic relationship of $\log K = A + \frac{B}{T} + \frac{C}{T^2}$ as determined by Van Arkel et al yielded an extrapolated value at the melting point of $K = 2.17 \times 10^{-4} \text{ ohm}^{-1} \text{ cm}^{-1}$ as previously indicated. The present investigation indicates that the linear relationship is probably more correct in the temperature range of the present investigation. It is possible that the discrepancy between the two results is due to a combination of factors such as the cell material, conductivity bridge used and cell design differences from the present arrangement.

DISCUSSION OF RESULTS

The addition of one mole % Na_2O to the boric oxide calls for an explanation. Boric oxide has a very poor conductivity and the range of the conductivity bridge used during the study is not sufficient to detect the conductivity of pure B_2O_3 . However addition of 1 mole % Na_2O to the boric oxide increases its conductivity by more than ten times. By maintaining a fixed mole fraction of 0.01 Na_2O to 0.99 B_2O_3 , it is clearly possible to study the electrical conductivity variation as a function of the variation of the vanadia content.

The magnitude of the electrical conductivity of the low vanadia samples (K is of the order of $10^{-4} \text{ohm}^{-1} \text{cm}^{-1}$) clearly indicates that the Na_2O alters only the structure of boric oxide. In fact, the entire sodium oxide addition modifies the network structure of boric oxide by breaking down the B-O linkage. Moreover, the initial addition of V_2O_5 can also be seen to have a similar effect, as pointed out later while considering the variation of the specific conductivity with vanadia content.

A. Variation of Specific Conductivity with mole % V_2O_5

Table 3 and Fig. 4 give $\log_{10}K$ vs. mole % V_2O_5 relationships at two temperatures 700°C (1) and 800°C (2). The two curves clearly indicate the same trend in the variation of specific conductivity with mole % V_2O_5 . The specific conductivity increases with the initial small additions of V_2O_5 as revealed by the change in the $\log_{10}K$ isotherms from 0 to 0.17 mole % V_2O_5 . Further additions of vanadium pentoxide do not increase the specific conductivity, at constant temperature, up to 20 mole % V_2O_5 . From 20 to 40 mole % V_2O_5 , the specific conductivity increases vary sharply with V_2O_5 content, at constant temperature. The increase becomes more gradual between 40 and 55 mole % V_2O_5 . The specific conductivity decreases with V_2O_5 content between 55 and 75 mole % V_2O_5 and then increases between 75 and 100 mole % V_2O_5 .

It is readily seen from the variation of $\log_{10}K$ with mole % V_2O_5 that:

1. V_2O_5 has a modifying action on the boric oxide network structure for the first small additions of V_2O_5 up to 0.1 mole %.
2. The sudden change in the specific conductivity at constant temperature between 20 and 40 mole % V_2O_5 indicates compound separation or liquid-liquid miscibility gap. The fact that the specific conductivity remains relatively constant between 0.1 to 20 mole % V_2O_5 supports the possibility of a miscibility gap.

TABLE 3
 VARIATION OF $\log_{10} K$ WITH MOLE % V_2O_5

At $\frac{700^\circ\text{C}}{K}$

Mole % V_2O_5	$\text{ohm}^{-1} \text{cm}^{-1}$	$\log_{10} K$
0.50	5.886×10^{-5}	$\bar{5}.7698$
0.17	1.420×10^{-4}	$\bar{4}.1523$
3.00	1.604×10^{-4}	$\bar{4}.2054$
13.60	1.968×10^{-4}	$\bar{4}.2941$
20.00	2.211×10^{-4}	$\bar{4}.3446$
25.00	6.701×10^{-4}	$\bar{4}.8261$
30.00	1.705×10^{-3}	$\bar{3}.2377$
37.00	3.193×10^{-3}	$\bar{3}.5041$
46.47	8.128×10^{-3}	$\bar{3}.9100$
60.39	1.749×10^{-2}	$\bar{2}.2428$
73.00	1.620×10^{-2}	$\bar{2}.2095$
88.00	1.05×10^{-2}	$\bar{2}.0212$
95.00	1.953×10^{-2}	$\bar{2}.2907$
100.00	3.100×10^{-2}	$\bar{2}.4914$

At $\frac{800^\circ\text{C}}{K}$

0	2.670×10^{-4}	$\bar{4}.4265$
0.17	4.893×10^{-4}	$\bar{4}.6895$
3.0	5.678×10^{-4}	$\bar{4}.7542$
13.6	5.761×10^{-4}	$\bar{4}.7605$
20.0	6.082×10^{-4}	$\bar{4}.7841$
25.0	1.301×10^{-3}	$\bar{3}.1142$
30.0	2.704×10^{-3}	$\bar{3}.4319$
37.0	1.132×10^{-2}	$\bar{2}.0539$
46.47	2.557×10^{-2}	$\bar{2}.4077$
60.39	4.108×10^{-2}	$\bar{2}.6136$
73	4.268×10^{-2}	$\bar{2}.6302$
88	3.0132×10^{-2}	$\bar{2}.4790$
95	4.337×10^{-2}	$\bar{2}.6372$
100	7.000×10^{-2}	$\bar{2}.8451$

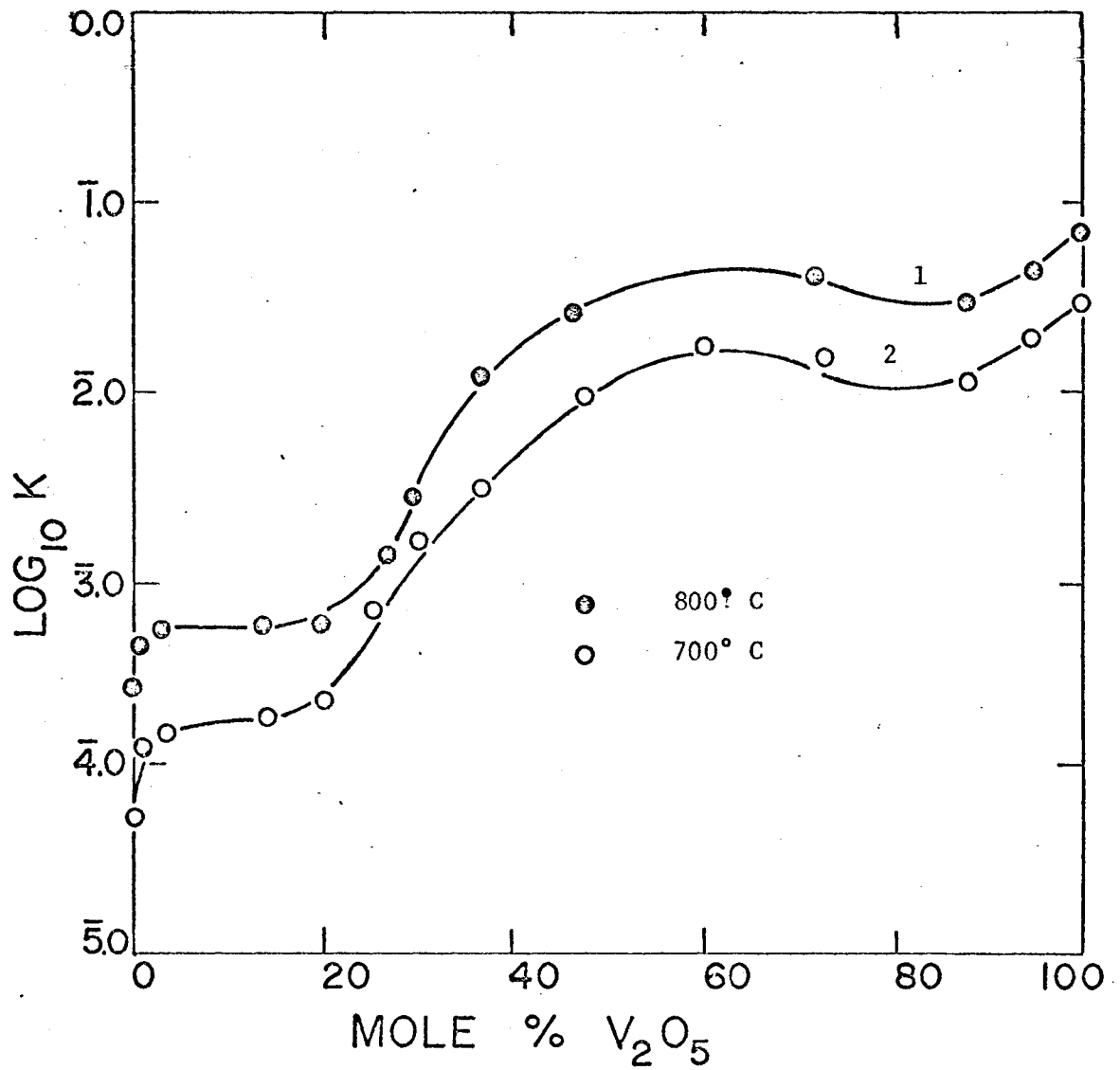


FIG. 4 $\text{LOG}_{10} K$ VS. MOLE % V_2O_5 RELATIONSHIP

3. The maxima and minima at 55 and 75 mole % V_2O_5 respectively in the $\log_{10}K$ isotherms are an interesting observation. This aspect is discussed later when considering the variation of E_k with mole % V_2O_5 .

B. Variation of Molar Conductivity with Mole % V_2O_5

Table 4 and Fig. 5 give the isothermal relationships of $\log_{10} \Lambda_M$ vs. mole % V_2O_5 where Λ_M is the molar conductivity. The trend is identical with the $\log_{10}K$ vs. mole % V_2O_5 plot except that there is a slight increase in the molar conductivity between 0.1 and 20 mole per cent V_2O_5 and that the decrease of molar conductivity between 55 and 75 mole % is less pronounced. It is readily apparent that this is due to the occurrence of the molecular weight M in the molar conductivity calculations.

C. Electrical Conductivity and Phase Separation

As pointed out earlier, the electrical conductivity data support the possibility of a liquid-liquid immiscibility region in the 0.1 to 20 mole % V_2O_5 composition region. An examination of the phase diagram determined previously by Nador (27) indicates however that such a phase separation should not occur. A closer scrutiny of the experimental procedure and the selected compositions in the determination of the phase diagram revealed that above 45 per cent by weight of B_2O_3 , the liquidus curve in the boric oxide rich region was in fact an extrapolation of the curve experimentally obtained for compositions in the vanadium

TABLE 4
 VARIATION OF $\log_{10} \Lambda_M$ WITH MOLE % V_2O_5

At 700°C

Mole % V_2O_5	Λ_M	$\log_{10} \Lambda_M$
0	25.2980×10^{-4}	$\bar{3}.4030$
0.17	56.9390×10^{-4}	$\bar{3}.7554$
3	73.0110×10^{-4}	$\bar{3}.8634$
13.6	93.379×10^{-4}	$\bar{3}.9703$
20	115.969×10^{-4}	$\bar{2}.0645$
25	36.109×10^{-3}	$\bar{2}.5576$
30	96.50×10^{-3}	$\bar{2}.9845$
37	20.044×10^{-2}	$\bar{1}.3104$
46.47	63.661×10^{-2}	$\bar{1}.8039$
60.30	142.015×10^{-2}	0.1523
73	147.8×10^{-2}	0.1697
88	110.10×10^{-2}	0.0418
95	200.938×10^{-2}	0.3029
100.	342×10^{-2}	0.5340

At 800°C

0	115.2679×10^{-4}	$\bar{2}.0615$
0.17	192.5132×10^{-4}	$\bar{2}.2844$
3	258.83×10^{-4}	$\bar{2}.4130$
13.6	287.263×10^{-4}	$\bar{2}.4583$
20	319.19×10^{-4}	$\bar{2}.5041$
25	72.2813×10^{-3}	$\bar{2}.8590$
30	151.182×10^{-3}	$\bar{1}.1796$
37	67.735×10^{-2}	$\bar{1}.8309$
46.47	178.591×10^{-2}	0.2519
60.39	335.72×10^{-2}	0.5259
73	391.618×10^{-2}	0.5929
88	317.382×10^{-2}	0.5015
95	460.178×10^{-2}	0.6630
100	795.063×10^{-2}	0.9004

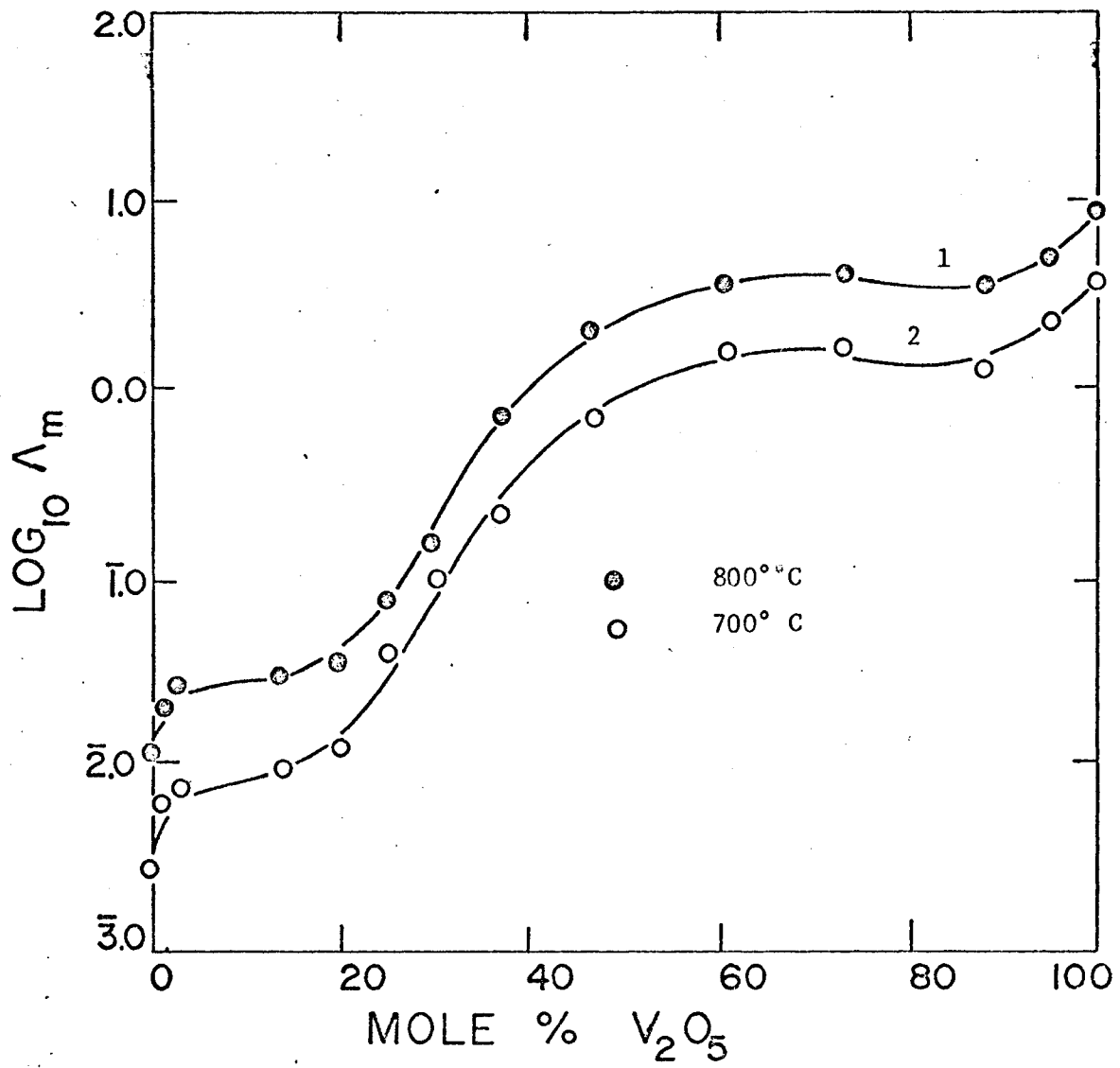


FIG. 5 $\text{LOG}_{10} \Lambda_m$ VS. MOLE % V_2O_5 RELATIONSHIP

pentoxide-rich region. This extrapolation could not be taken for granted in view of the wide region of composition over which the extrapolation was made with no experimental points in the extrapolated region.

D. Visual Examination

A mere visual examination of the melts of boric oxide containing 1 to 10 mole % V_2O_5 reveals layers of two liquids in the platinum crucible. The bottom layer can easily be seen through the upper layer. The second phase can be distinctly seen even after solidification.

Thus the system $B_2O_3 - V_2O_5$ shows a liquid-liquid miscibility gap between 0.1 and 20 mole % V_2O_5 as indicated by the conductivity data.

E. Monotectic Temperature

Having thus established the existence of a monotectic region in the system $B_2O_3 - V_2O_5$, the monotectic temperature determined was used to modify the phase diagram.

The break at $593 \pm 5^\circ C$ in all the compositions in Fig. 6 was positive proof of the miscibility gap in the system. Fig. 7 is the modified phase diagram incorporating the liquid-liquid miscibility gap region. No attempt was made to check the experimentally determined liquidus points in the existing phase diagram. The intersection of the monotectic temperature horizontal with the existing liquidus curve

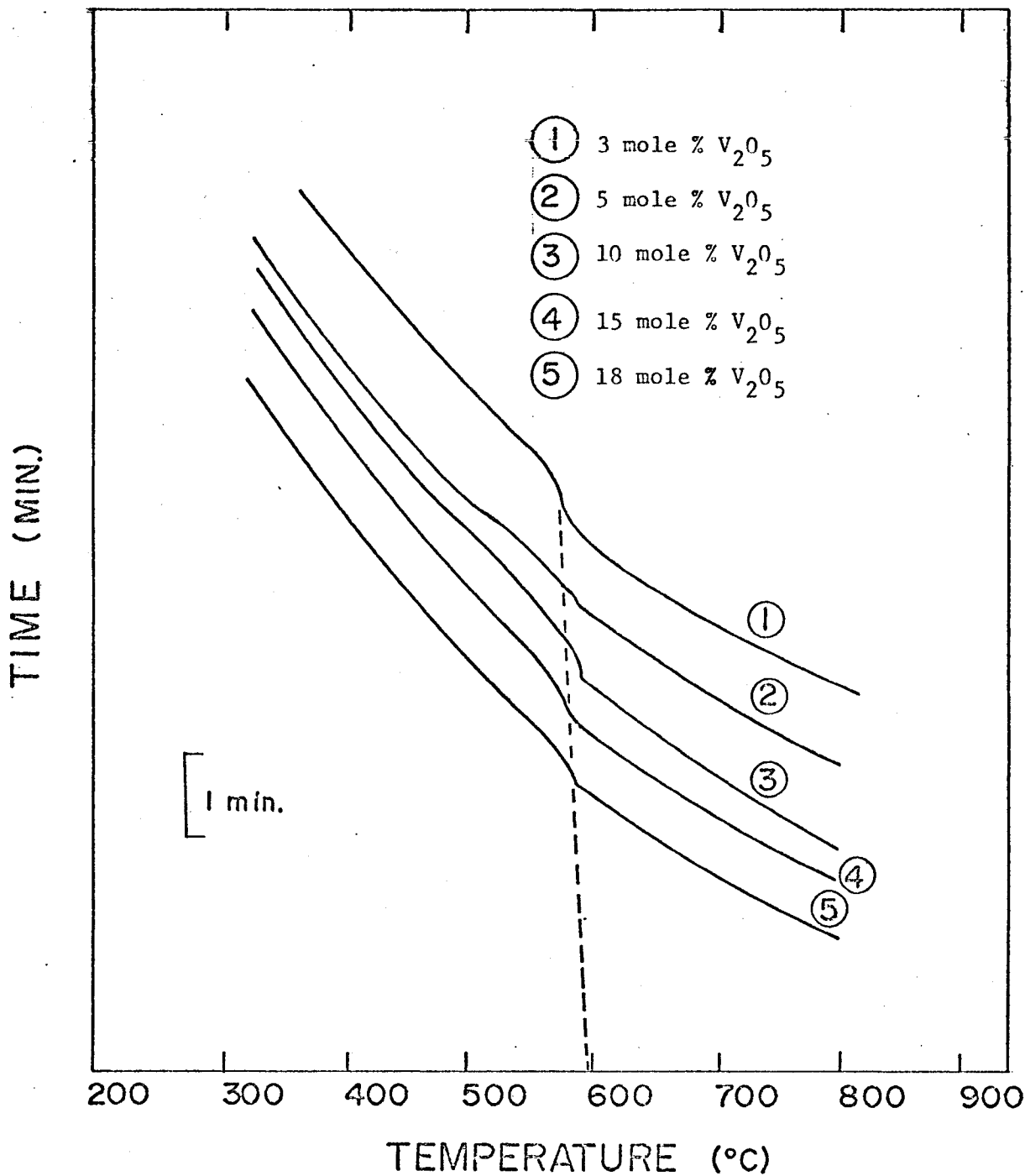


FIG. 6 COOLING CURVES AT MONOTECTIC
COMPOSITION REGION

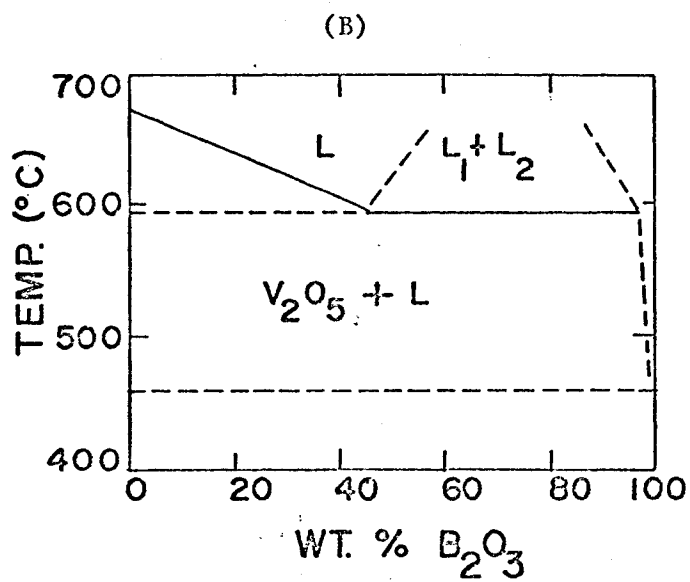
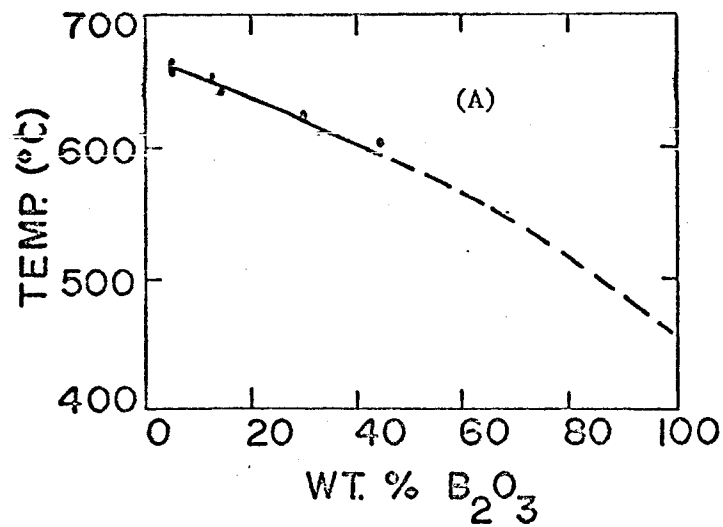


FIG. 7 PHASE DIAGRAM OF $B_2O_3 - V_2O_5$ SYSTEM

(A) FROM REF. 27

(B) MODIFIED PHASE DIAGRAM

determines the limiting composition of immiscibility and is in agreement with the observed conductivity change in the system above 20 mole % V_2O_5 .

F. Examination of Immiscibility

Levin examines the principles of structural interpretation of immiscibility in oxide systems (31). Taking ionic field strength as

$$IFS = \frac{Z}{(r + 1.40)^2}$$

Levin postulates that if the Δ IFS obtained by subtracting IFS of the modifier ion with the oxygen ion from the IFS of the glass former cation with oxygen ion is a measure of liquid immiscibility in a binary oxide system. If the Δ IFS value so obtained is in the range from 0.8 to 0.06 approximately, immiscibility should occur.

$$\text{For the vanadium ion } V^{5+}, \quad \begin{array}{l} z = 5 \\ r = 0.59 \end{array}$$

$$\text{Hence } IFS_{V^{5+}} = \frac{5}{(0.59 + 1.40)^2} = 1.263$$

and for the boron ion B^{3+}

$$\begin{array}{l} z = 3 \\ r = 0.23 \end{array}$$

$$IFS_{B^{3+}} = \frac{3}{(0.23 + 1.60)^2} = 1.129$$

subtracting $IFS_{V^{5+}}$ from $IFS_{B^{3+}}$

$$\Delta IFS = -0.134$$

No immiscibility should occur with boron as the glass forming cation and vanadium as modifier ion. However there is positive evidence of immiscibility. On the other hand there should be immiscibility in the other end of the system, as the value of $IFS_{V^{5+}} - IFS_{B^{3+}} = 0.134$; no immiscibility has however been observed.

Thus vanadia systems, generally known to be exceptions to the ionic field strength concept and other concepts of immiscibility, add more confusion by the present observation of immiscibility in the boric oxide rich composition region.

G. Variation of E_k with Mole % V_2O_5 and the Conductivity Changes from 0 to 100 Mole % V_2O_5

The $\log_{10}K$ vs. $\frac{1}{T}$ relationships of all the samples (Figs. 8 to 21) are linear. The activation energy E_k of each composition is evaluated from the slope of the $\log_{10}K$ vs. $\frac{1}{T}$ straight lines.

Table 5 and Fig. 8 give the relationship of E_k vs. mole % V_2O_5 . It is instructive to compare this with similar plots in other systems.

Bockris and Mellors (10) had plotted E_k vs. mole % PbO in the system $B_2O_3 - PbO$. The E_k value shows a gradual decrease from 100 mole % PbO to about 75% mole PbO followed by an increase below 75% mole PbO.

They explained the trend as (1) up to 75 mole % PbO, only planar BO_3 ions exist (2) between 75 and 50 mole % PbO straight chains of $-O-\overset{\overset{O}{\parallel}}{B}-O-B-O$ type form (3) below 50 mole % PbO, $-B-O-B-$ bonds are broken for Pb^{++} to find easier passage between interstices, as pointed out earlier.

Comparison of the plot of E_k vs. mole % XO in the $PbO - B_2O_3$ and $B_2O_3 - V_2O_5$ systems reveals distinct differences.

TABLE 5
 ACTIVATION ENERGY OF CONDUCTANCE AT
 DIFFERENT COMPOSITIONS

Mole %	Slope x 10 ⁻⁴	Activation Energy of Conductance k cal/mole
0	0.57895	26.458
0.17	0.52381	23.938
3	0.53398	24.403
13.6	0.45833	20.946
20	0.44898	20.518
25	0.33333	15.233
30	0.22449	19.259
37	0.52381	23.938
46.47	0.44898	20.518
60.39	0.39568	18.083
73	0.59026	23.273
88	0.46809	21.3917
95	0.366607	16.7568
100	0.36667	16.7568

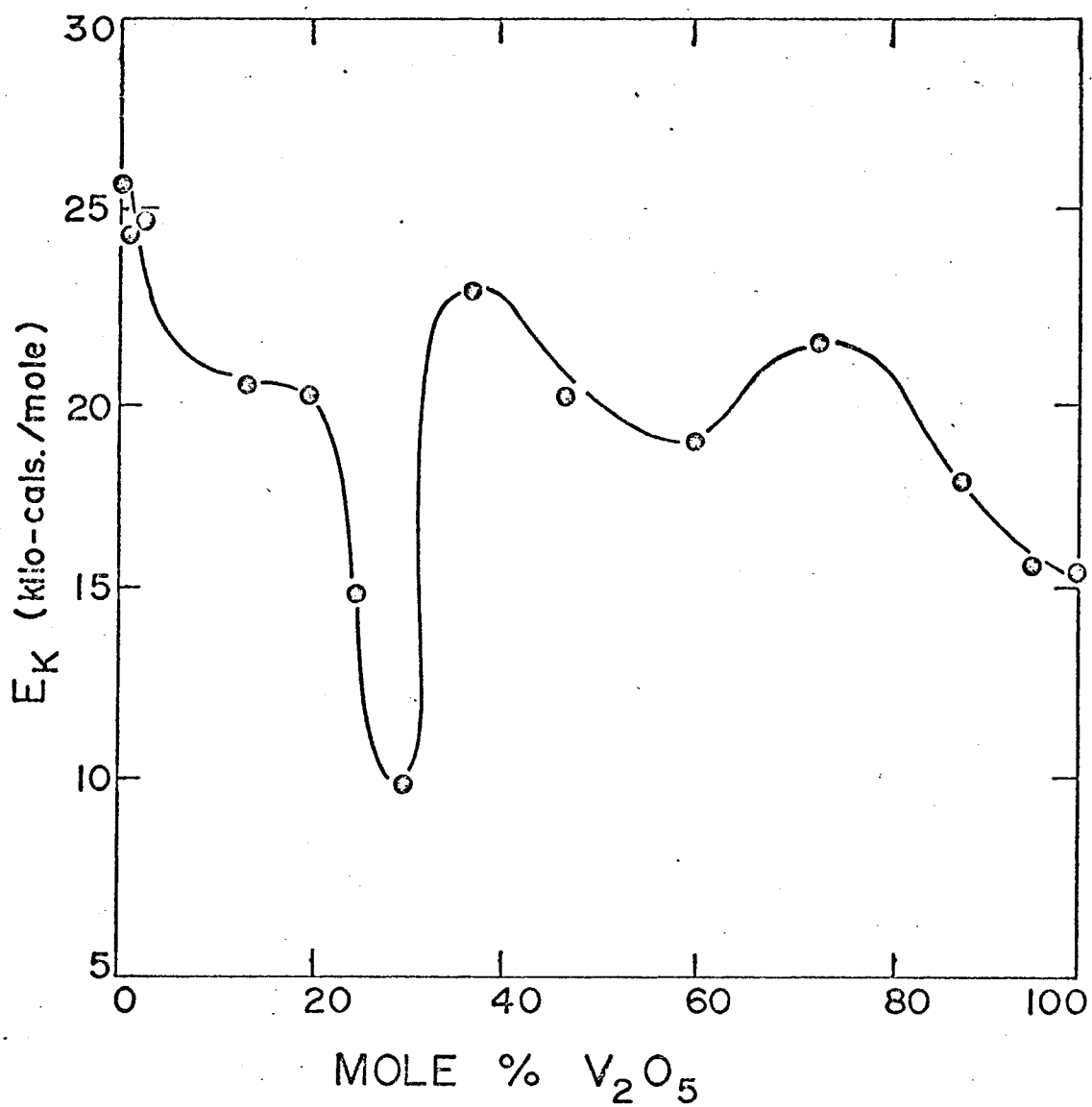


FIG. 8 ACTIVATION ENERGY OF CONDUCTANCE E_k VS.
MOLE % V_2O_5 RELATIONSHIP

In E_k vs mole % V_2O_5 curve, the E_k value decreases with the first additions of V_2O_5 , levels off with further additions up to 20 mole % and then there is a sharp drop up to 30 mole % V_2O_5 . The E_k then increases sharply up to 37 mole % V_2O_5 , decreases up to 55 mole % V_2O_5 , again increases up to 75 mole % V_2O_5 and then decreases to 100 mole % V_2O_5 .

Considering the variation of E_k with mole % V_2O_5 from the V_2O_5 end, the vanadium ion in V_2O_5 is reported to be five-coordinated with oxygen (31). The gradual addition of B_2O_3 probably shifts the structure to octahedral coordination. Vanadium has been reported to exist in octahedral coordination in KV_3O_8 and $C_sV_3O_8$ (29). Stoichiometrically this would imply octahedral coordination at about 75 mole % V_2O_5 in the $K_2O - V_2O_5$ system. The increase of activation energy E_k with the gradual addition of B_2O_3 may therefore be justifiably attributed to the change from five coordination to octahedral coordination of the vanadium ion with oxygen. The fact that the E_k maxima occurs at the 75 mole % composition approximately, supports this interpretation. The specific and molar conductivity minima at 75 mole % V_2O_5 are also thus explained satisfactorily.

The increase in the specific and molar conductivities between 75 and 55 mole % V_2O_5 and the corresponding decrease of activation energy E_k in this composition range may perhaps be due to a partial shift of the octahedral coordination to tetrahedral coordination. As has been

pointed out earlier, vanadium has been reported to exist in tetrahedral coordination in NaVO_3 corresponding to 50 mole % V_2O_5 in the system $\text{Na}_2\text{O} - \text{V}_2\text{O}_5$. The fact that the E_k minima, the $\log_{10} K$ and $\log_{10} \Lambda_M$ maxima occurs at about 55 mole % V_2O_5 lends support to this interpretation.

The increase of E_k between 55 and 37 mole % V_2O_5 and the corresponding gradual decrease in specific and molar conductivities may be attributed to the straight chains of $-\text{O}-\overset{\text{O}}{\underset{\text{O}}{\text{B}}}-\text{O}-\dots$ type groups as postulated by Bockris and Mellors (10). The existence of a $\text{BO}_3 \rightleftharpoons \text{BO}_4$ equilibrium in the melt does not preclude the formations of straight chains as above, in view of the fact that the decreasing oxide content (i.e. V_2O_5 in this case) in B_2O_3 should favour BO_3 configuration, as mentioned earlier.

The sharp fall in the value of E_k from 37 mole % to 30 mole % V_2O_5 is due to the introduction of an immiscible phase. The rise of E_k up to 20 mole % V_2O_5 is probably due to the change in position of the liquid-liquid interface which, in this region of composition, should meet the electrodes. If this interpretation is correct, the region of constant E_k is due to liquid-liquid immiscibility where the liquid-liquid interface is below the level of electrodes. The further rise of E_k with B_2O_3 up to the base mixture is due to the modifying action of V_2O_5 in boric oxide (i.e. the "net work-breaking" effect of V_2O_5 on B_2O_3).

The existence of liquid-liquid immiscibility prevents the possible formation of the type of rings as proposed by Bockris and Mellors (10) in $\text{PbO} - \text{B}_2\text{O}_3$ system.

One of the essential conditions of liquid-liquid immiscibility, as postulated by Levin, is that liquid-liquid immiscibility occurs in binary glass forming oxide systems, only if the glass forming cation is three or four coordinated with oxygen and the modifying cation is six or more coordinated. The absence of immiscibility in the V_2O_5 rich region is due to the fact V^{5+} does not exist as three or four coordinated only in that region. The interpretation of octahedral coordination is supported by this coincidence. The existence of immiscibility at the boric oxide rich region indicates that V^{5+} should be six or more coordinated in that region. It is easy to see why only a partial shift to tetrahedral coordination is postulated in the explanation for the variation of E_k from 75 mole % to 55 mole % V_2O_5 .

CONCLUSIONS

The study has thus revealed many interesting aspects of the $B_2O_3 - V_2O_5$ system. It has been postulated that the variation in the specific and molar conductivities with increasing V_2O_5 content is dependent on the phase relationships in the system and the nature of the vanadium ion. Thus, the initial conductivity increases up to 0.1 mole % V_2O_5 corresponds to the modifying action of V_2O_5 on the B_2O_3 network structure. The region of constant specific and molar conductivities (ie. 0.1 to 20 mole % V_2O_5) is due to the occurrence of liquid-liquid immiscibility in the system $V_2O_5 - B_2O_3$ in that composition region. The sharp increase in the conductivities between 20 and 35 mole % V_2O_5 indicates a change from liquid immiscibility to miscibility. Further conductivity changes are due to the change in the nature of the vanadium ion. Thus, the vanadium ion is capable of assuming tetrahedral and octahedral coordination configurations with oxygen in addition to the five coordination configuration as in the pure liquid V_2O_5 .

As a result of the study, the existing phase diagram of the system $B_2O_3 - V_2O_5$ has been modified. A modified phase diagram, incorporating the monotectic region in the system, has been drawn up.

The occurrence of liquid-liquid immiscibility in the B_2O_3 rich region has revealed that the system behaves as an exception to the existing concepts of liquid-liquid immiscibility.

The intersection of the monotectic temperature horizontal with the liquidus curve determines the limiting composition of immiscibility as 45 weight % B_2O_3 in the $B_2O_3 - V_2O_5$ system. The monotectic temperature has been determined as $593 \pm 5^\circ C$.

The variation of the conductivity with increasing vanadia contents and the magnitude of the specific conductivity near to the melting point (i.e. $K = 3.10 \times 10^{-2} \text{ohm}^{-1} \text{cm}^{-1}$ at $700^\circ C$) has clearly established that liquid vanadia is ionic in nature.

The variation of activation energy of conductance E_k with increasing mole % V_2O_5 also supports the occurrence of liquid-liquid immiscibility and the change in the coordination configuration of the vanadium ion with oxygen in the melts.

REFERENCES

1. Tichanowitsch, M. "Electrical Conductivity Characteristics of some liquid oxides" Chem Zentr. (11) 6:613, (1861)
2. Arndt, K and Gessler, A, "Electrical Conductivity Studies in liquid Boron Trioxide", Z. Electrochem 14:622, (1908)
3. Shartsis, L. Capps, W. and Spinner S., "Viscosity and Electrical Resistivity of Molten Alkali Borates", J. Amer. Cera. Soc. 36, 319 (1953)
4. J.D. Mackenzie, "The Viscosity Molar Volume and Electrical Conductivity of liquid Boron Trioxide", Trans. Farad. Soc. 52, 1564 (1956)
5. J.D. Mackenzie, "Energy of the B-O bond and the Structure of liquid Boron Trioxide", J. of Chem. Physics, 25, 187 (1956)
6. Shartsis, L., Capps, W. and Spinner, S., "Viscosity and Electrical Resistivity of molten Alkali Borates", J. of Amer. Chem. Soc. 36, 319 (1953)
7. J. Zarceki, "Coordination of Oxygen in liquid Boric Oxides at elevated temperatures by X-ray Diffraction", Proce. IV interna. Congress on Glass, Paris, VI, 323 (1956)
8. J.D. Mackenzie, "Structure of liquid Boron Trioxide", J. of Phys. Chem., 63, 1875 (1959)
9. D. White, P.N. Walsh and D. E. Mann, "Infrared Emission Spectra of B₂O₃ (g)", J. of Chem. Phys., 60, 1321, (1956)
10. Bockris and Mellors, "Electrical Conductivity Studies on PbO - SiO₂ and PbO - B₂O₃ Systems", J. Phys. Chem., 60, 1321, (1956)
11. J.D. Mackenzie, "Structure of Some Inorganic Glasses from High Temperature Studies of Binary Borates", "Modern Aspects of the Vitreous State", Butterworths Publications, 1, 215 (1960)
12. Levin, E.M. and Block, S., "Structural Interpretation of Immiscibility in Oxide Systems", II, "Coordination Principles Applied to Immiscibility", J. Amer. Ceram. Soc., 40, 113, (1957)

13. Fajans and S.W. Barber, "Properties and Structures of Vitreous and Crystalline Boron Oxide", J. of Amer. Chem. Society, 74, 2761, (1952)
14. S.L. Anderson, R.L. Bohn and D.D. Kimpton, "Infrared Spectra and Atomic Arrangement in Fused Boron Oxide and Soda Borate Glasses", J. Amer. Cer. Soc., 38, 370 (1955)
15. B.E. Warren, H. Krutter and O. Morningstar, "Fourier Analysis of X-ray Patterns of Vitreous SiO₂ and B₂O₃", J. Amer. Cer. Soc., 38, 370 (1936)
16. Weyl and Marboe, "Constitution and Properties of some Representative Glasses", "The Constitution of Glasses: an Interscience Publication, Vol. II, Part 1, 540 (1964)
17. G.W. Stewart, "Structure and Molecular Forces in Pure Liquids", J. of Phys. 12, 321 (1964)
18. V.V. Tarsov, "Polymer Models and Properties of Boric Anhydride and Borate Glasses", "The Structure of Glass" (Translated from Russian), Consultants Bureau, N.Y., 6, 17 (1966)
19. Berger, J.V., "Crystal Structure of Boron Trioxide", Acta Chem. Scand., 7, 611 (1953)
20. Inorganic Index to the Powder Diffraction File, 1968, ASTM Publication PDIS-18i, Page 497
21. Powder Diffraction File Card No. 6-0297, Inorganic Index to the Powder Diffraction File, ASTM Publication, PDIS-18i, 497 (1968)
22. Buff, H., "Electrical Conductivity of Molten V₂O₅", Liebigs Ann Chem., 110, 257, (1859)
23. A.E. Van Arkel, E.A. Flood, and N.A.H. Bright, "Electrical Conductivities of Molten Oxides", Canadian Journal of Chemistry, 31, 1009 (1953)
24. "Crystal Structure of Vanadium Pentoxide", Nat. Bureau of Standards Circ., 8, 539, (1958)
25. Inorganic Index to the Powder Diffractions File, ASTM Publications PDIS-18i, 590 (1968)
26. J.D. Mackenzie, "Structure of Some Inorganic Glasses from High High Temperature Studies: Pure Oxides", "Modern Aspects of the Vitreous State", London Butterworths Publication, Vol. I, 192 (1960)

27. B. Nador, "Phase Diagram of the System $B_2O_3 - V_2O_5$ ", *Nature*, 188, 139, (1966)
28. E.M. Levin, "Structural Interpretations of Immiscibility in Oxide Systems: IV, Occurrence, Extent and Temperature of the Monotectic", *J. of Amer. Cer. Soc.*, 36, 50, (1967)
29. Stanley Block: "Crystal Structure of Potassium Tri Vanadate", *Nature*, 186, 540, (1960)
30. H.T. Evans, Jr., "Crystal Structure Refinement and Vanadium Bonding in the Meta Vanadates KVO_3 , NH_4VO_3 and $KVO_3 \cdot H_2O$ ", *Z. Krist.*, 114, 257-277 (1960)
31. E.M. Levin, "Structural Interpretation of Immiscibility in Oxide Systems: IV Occurrence, Extent and Temperature of the Monotectic", *J. Amer. Cer. Soc.*, 37, 50, (1967)
32. Mackenzie, J.D. , "The Physical Chemistry of Simple Molten Glasses", *Chem. Review*, 56, 458 (1956)

APPENDIX-1

CONDUCTIVITY DATA AND CALCULATIONS

TABLES 6 TO 20

TABLE 6
Electrical Conductivity data of
Sample (1)

Base Mixture		Boric oxide with 1 mole % Na ₂ O					
Boric oxide		48.5533 gms.					
Sodium tetraborate		1.4470 gms.					
Depth of melt		6.2 Div. (1 Div. 0.02")					
C, Cell constant		1.09 cm ⁻¹ (from chart)					
Mol. Weight M.		69.653					
Room temp volume corresponding to melt height		30cc. (from chart)					
Temp. °C	G_M Measured Conductivity ohms ⁻¹	Temp. T°K	$\frac{1}{T} \times 10^3$	K sp. conductivity ohm ⁻¹ cm ⁻¹	V_B Volume of Melt cc	ρ_B Density of Melt gms/cc	$\Lambda_M \times 10^4$ Molar Conductivity x 10 ⁴ ohm ⁻¹ mole ⁻¹ cm ²
							$\frac{K M}{\rho_B}$
859	4.46x10 ⁻⁴	1132	0.88339	4.8614x10 ⁻⁴	31.0952	1.6080	210.3069
851	4.04x10 ⁻⁴	1124	0.88967	4.4036x10 ⁻⁴	31.0850	1.6085	190.4430
844	3.75x10 ⁻⁴	1117	0.89525	4.0875x10 ⁻⁴	31.0761	1.6090	176.7177
842	3.68x10 ⁻⁴	1115	0.89686	4.0112x10 ⁻⁴	31.0736	1.6091	173.4082
837.20	3.60x10 ⁻⁴	1110.20	0.90090	3.9024x10 ⁻⁴	31.0674	1.6094	179.6068
827	3.20x10 ⁻⁴	1100	0.90991	3.488x10 ⁻⁴	31.0544	1.6100	150.7055
822	3.12x10 ⁻⁴	1095	0.91324	3.400x10 ⁻⁴	31.0480	1.6104	146.8667
807.5	2.67x10 ⁻⁴	1080.5	0.92550	2.9103x10 ⁻⁴	31.0296	1.6114	125.6355
800	2.45x10 ⁻⁴	1070	0.93196	2.6705x10 ⁻⁴	31.020	1.6119	115.2479
788	2.18x10 ⁻⁴	1061	0.94250	2.3762x10 ⁻⁴	31.0047	1.6127	102.4962
783	2.03x10 ⁻⁴	1056	0.94696	2.2672x10 ⁻⁴	30.9983	1.6130	97.7632
740	1.21x10 ⁻⁴	1013	0.98716	1.3189x10 ⁻⁴	30.9435	1.6158	56.7810
732	1.10x10 ⁻⁴	1005	0.99502	1.199x10 ⁻⁴	30.9333	1.6164	51.9991
700	0.54x10 ⁻⁵	973	1.0277	0.5886x10 ⁻⁵	30.8925	1.6185	25.2980
658	3.64x10 ⁻⁵	931	1.0761	3.9676x10 ⁻⁵	30.8390	1.6213	17.0233
648	3.00x10 ⁻⁵	921	1.0857	3.27x10 ⁻⁵	30.8262	1.6220	14.0241

TABLE 7
Electrical Conductivity data of
Sample (2)

0.17 mole percent V_2O_5
Base Mixture + 0.2267 gms of V_2O_5
Depth of melt 6 Div.
C, Cell constant 1.06
Mol. Weight M = 69.8308
Room temp volume corresponding to melt height 28cc

Temp °C	G_M Measured Conductivity ohms ⁻¹	Temp. T°K	$\frac{1}{T} \times 10^3$	K sp. conductivity ohm ⁻¹ cm ⁻¹	V_2 Volume of melt cc	ρ_2 Density of Melt gms/cc	$\Lambda_M \times 10^4$ Molar Conductivity x 10 ⁴ ohm ⁻¹ mole ⁻¹ cm ²
859	7.7×10^{-4}	1132	0.88339	8.162×10^{-4}	29.0222	1.7306	329.3418
855	7.44×10^{-4}	1128	0.88652	7.8864×10^{-4}	29.0715	1.7309	318.1661
851	7.12×10^{-4}	1124	0.88967	7.5472×10^{-4}	29.0127	1.7312	304.4288
838	6.4×10^{-4}	1111	0.90009	6.786×10^{-4}	28.9972	1.7321	273.3565
823	5.72×10^{-4}	1096	0.91240	6.0632×10^{-4}	28.9794	1.7332	244.3653
815	5.28×10^{-4}	1088	0.91911	5.5968×10^{-4}	28.9699	1.7338	225.4176
804	4.73×10^{-4}	1077	0.92850	5.0138×10^{-4}	28.9568	1.7345	201.8551
801	4.56×10^{-4}	1074	0.93109	4.8124×10^{-4}	28.9532	1.7348	193.7132
796	4.36×10^{-4}	1069	0.93545	4.6216×10^{-4}	28.9472	1.7351	186.0008
788	4.1×10^{-4}	1061	0.94251	4.346×10^{-4}	28.9377	1.7357	174.8486
740	2.29×10^{-4}	1013	0.98716	2.4276×10^{-4}	28.8806	1.7391	97.5486
730	2.04×10^{-4}	1003	0.99700	2.1624×10^{-4}	28.8682	1.7398	86.7950
722	1.85×10^{-4}	995	1.0050	1.9610×10^{-4}	28.8592	1.7404	78.6821
716	1.68×10^{-4}	989	1.0111	1.7808×10^{-4}	28.8520	1.7608	71.4354
700	1.36×10^{-4}	973	1.0277	1.4204×10^{-4}	28.833	1.7620	56.9390

TABLE 8
Electrical Conductivity data of
Sample (3)

3 mole per cent V_2O_5

Base Mixture	3.7689 gms. V_2O_5
Depth of melt	6 Div.
C, Cell constant	1.12
Molecular Weight	72.9325
Room temp volume corresponding to melt height	32.5cc.

Temp. °C	G_M Measured Conductivity ohm ⁻¹ s	Temp. T °K	$\frac{1}{T} \times 10^3$	K Sp. conductivity ohm ⁻¹ cm ⁻¹	V_3 Volume of melt cc	ρ_3 Density of Melt gms/cc	$\Lambda_M \times 10^4$ Molar Conductivity x 10 ⁴ ohm ⁻¹ mole ⁻¹ cm ²
859	8.7×10^{-4}	1192	0.88339	9.744×10^{-4}	33.6864	1.5962	445.2163
851	7.98×10^{-4}	1124	0.88967	8.9876×10^{-4}	33.6754	1.5967	408.2430
844	7.48×10^{-4}	1117	0.89525	8.3776×10^{-4}	33.6658	1.5971	382.5680
814	5.85×10^{-4}	1087	0.91996	6.5520×10^{-4}	33.6245	1.5991	298.827
804	5.3×10^{-4}	1077	0.92850	5.9360×10^{-4}	33.6105	1.5998	270.6134
796	4.84×10^{-4}	1069	0.93545	5.4208×10^{-4}	33.5995	1.6003	247.049
787	4.47×10^{-4}	1060	0.94339	5.0064×10^{-4}	33.5871	1.6008	228.092
726	2.18×10^{-4}	999	1.0010	2.4416×10^{-4}	33.5279	1.6037	111.038
707	1.66×10^{-4}	980	1.0206	1.8592×10^{-4}	33.4766	1.6061	84.43
697	1.36×10^{-4}	970	1.0309	1.5008×10^{-4}	33.4627	1.6068	68.121
673	1.04×10^{-4}	946	1.0570	1.1648×10^{-4}	33.4296	1.6084	52.818
655	0.75×10^{-4}	928	1.0775	0.84×10^{-4}	33.4047	1.6096	38.0612
616	0.364×10^{-4}	889	1.1248	0.40768×10^{-4}	33.3509	1.6122	18.4426

TABLE 9
Electrical Conductivity data of
Sample (4)

13.6 mole per cent V_2O_5	
Boric oxide B_2O_3	33.9561 gms.
Sodium tetraborate $Na_2B_4O_7$	1.0118 gms.
Vanadium Pentoxide V_2O_5	14.4085 gms.
Depth of Melt	5.8
Cell constant	1.04
Mol. Weight	84.8381
Room temp volume corresponding to melt height	27.5cc.

Temp. °C	G_M Measured Conductivity $ohm^{-1}s$	Temp T °K	$\frac{1}{T} \times 10^3$	K sp. conductivity $ohm^{-1}cm^{-1}$	V_4 Volume of melt cc	ρ_4 Density of Melt gms/cc	$\Lambda_M \times 10^4$ Molar Conductivity $\times 10^4$ $ohm^{-1}mole^{-1}cm^2$
859	9.1×10^{-4}	1132	0.88339	9.4635×10^{-4}	28.5060	1.6976	472.98
847	8.12×10^{-4}	1120	0.89285	8.4444×10^{-4}	28.4900	1.6983	421.389
820	6.48×10^{-4}	1093	0.91491	6.7388×10^{-4}	28.4584	1.7001	335.28
807	5.93×10^{-4}	1080	0.92592	6.1669×10^{-4}	28.4433	1.7010	307.58
800	5.56×10^{-4}	1073	0.93196	5.7613×10^{-4}	28.4350	1.7015	287.263
773	4.34×10^{-4}	1046	0.95602	4.5134×10^{-4}	38.4034	1.7034	224.79
746	3.20×10^{-4}	1019	0.98135	3.3278×10^{-4}	28.3719	1.7053	165.59
710	2.08×10^{-4}	983	1.0172	2.1631×10^{-4}	28.3292	1.7079	107.45
692	1.59×10^{-4}	965	1.0362	1.6535×10^{-4}	28.3085	1.7091	82.079
656	0.98×10^{-4}	929	1.0764	1.0191×10^{-4}	28.2673	1.7116	50.516
627	0.606×10^{-4}	900	1.1111	6.3020×10^{-5}	28.2215	1.7166	31.186
593	0.306×10^{-4}	866	1.1547	3.182×10^{-5}	28.1930	1.7161	15.732

TABLE 10
Electrical Conductivity data of
Sample (5)

20 mole per cent V_2O_5		
Base Mixture	B_2O_3	35.8462
	$Na_2B_4O_7$	1.0737
	V_2O_5	22.9315
Melt height	6.6	
C, Cell constant	1.135	
Molar Weight	92.0264	
Room temp volume corresponding to the melt height		33cc.

Temp °C	G_M Measured Conductivity ohms ⁻¹	Temp. T°K	$\frac{1}{T} \times 10^3$	K sp. conductivity ohm ⁻¹ cm ⁻¹	V_5 Volume of Melt cc	ρ_5 Density of melt gms/cc	$\Lambda_M \times 10^4$ Molar Conductivity $\times 10^4$ ohm ⁻¹ mole ⁻¹ cm ²
859	8.56×10^{-4}	1132	0.88339	9.6929×10^{-4}	34.2047	1.7498	509.774
851	8×10^{-4}	1124	0.88967	9.080×10^{-4}	34.1935	1.7503	477.404
842	7.46×10^{-4}	1115	0.89686	8.4444×10^{-4}	34.1809	1.7510	443.81
822	6.46×10^{-4}	1095	0.91324	7.3321×10^{-4}	34.1529	1.7525	385.0196
807	5.60×10^{-4}	1080	0.92592	6.3560×10^{-4}	34.1319	1.7535	333.57
800	5.36×10^{-4}	1073	0.93196	6.0836×10^{-4}	34.1220	1.7540	319.19
772	4.20×10^{-4}	1045	0.95693	4.7670×10^{-4}	34.0824	1.7560	249.824
746	3.22×10^{-4}	1023	0.97751	3.6547×10^{-4}	34.0463	1.7579	191.324
726	2.61×10^{-4}	1003	0.99700	2.9623×10^{-4}	34.0182	1.7594	154.942
696	1.86×10^{-4}	969	1.0319	2.1111×10^{-4}	33.9768	1.7615	110.289
666	1.26×10^{-4}	939	1.0649	1.4301×10^{-4}	33.9339	1.7638	76.6153
633	0.79×10^{-4}	906	1.1037	0.8967×10^{-4}	33.8878	1.7662	46.719
614	0.58×10^{-4}	887	1.1273	0.6583×10^{-4}	33.8611	1.7676	34.273

TABLE 11
Electrical Conductivity data of
Sample (6)

25 mole per cent V_2O_5

B_2O_3 29.9498 gms.
 $Na_2B_4O_7$ 0.8455
26.8393 gms.

B_2O_3
Melt height 6.3 Div
C, Cell constant 1.1
Molar Weight 97.6423

Room temp volume corresponding to the melt height: 31cc.

Temp. °C	G_M Measured Conductivity ohm ⁻¹ s	Temp. T°K	$\frac{1}{T} \times 10^3$	K sp. conductivity ohm ⁻¹ cm ⁻¹	V_6 Volume of Melt cc	ρ_6 Density of melt gms/cc	$M \times 10^4$ Molar Conductivity $\times 10^4$ ohm ⁻¹ mole ⁻¹ cm ²
859	1.84×10^{-3}	1132	0.88339	2.024×10^{-3}	32.1312	1.7937	110.179
851	1.70×10^{-3}	1124	0.88967	1.870×10^{-3}	32.1212	1.7943	101.762
842	1.59×10^{-3}	1115	0.89686	1.749×10^{-3}	32.1093	1.7950	95.140
820	1.39×10^{-3}	1093	0.91491	1.5290×10^{-3}	32.0804	1.7966	83.099
807	1.28×10^{-3}	1080	0.92592	1.408×10^{-3}	32.0633	1.7975	76.484
800	1.21×10^{-3}	1073	0.93196	1.3310×10^{-3}	32.0540	1.7980	72.2813
771	0.9850×10^{-3}	1044	0.95785	1.0835×10^{-3}	32.0158	1.8000	58.7752
746	0.8×10^{-3}	1019	0.98135	0.8800×10^{-3}	31.9829	1.8020	47.6832
726	0.67×10^{-3}	999	0.99700	0.7370×10^{-3}	31.9565	1.8035	39.9015
697	0.60×10^{-3}	970	1.0309	0.66×10^{-3}	31.9183	1.8057	35.689
678	0.58×10^{-3}	951	1.0515	0.638×10^{-3}	31.8931	1.8071	34.473

TABLE 12
Electrical Conductivity data of
Sample (7)

30 mole per cent V_2O_5

	B_2O_3	20.4769 gms.
	V_2O_5	23.8089 gms.
	$Na_2B_4O_7$	0.5780 gms.
Depth of melt	5.2 Div.	
C, Cell constant	1.09	
Molar Weight	103.2581	
Room temp volume corresponding to melt height (from chart)		23.5cc.

Temp. °C	κ_M Measured Conductivity ohm ⁻¹	Temp. T°K	$\frac{1}{T^\circ K} \times 10^3$	K sp. conductivity ohm ⁻¹ cm ⁻¹	V_7 Volume of melt cc	Density of melt ρ_7 gms/cc	$\Lambda_M \times 10^4$ Molar Conductivity $\times 10^4$ ohm ⁻¹ mole ⁻¹ cm ²
859	3.34x10 ⁻³	1132	0.88339	3.64x10 ⁻³	24.3579	1.8419	204.00
851	3.23x10 ⁻³	1124	0.88967	3.5207x10 ⁻³	24.3499	1.8424	197.319
842	3.08x10 ⁻³	1115	0.89686	3.3572x10 ⁻³	24.3409	1.8431	188.084
827	2.88x10 ⁻³	1100	0.909091	3.1392x10 ⁻³	24.3260	1.8443	175.76
807	2.58x10 ⁻³	1080	0.92592	2.8122x10 ⁻³	24.3061	1.8458	157.32
800	2.48x10 ⁻³	1073	0.93596	2.7032x10 ⁻³	24.2990	1.8463	151.182
776	2.18x10 ⁻³	1049	0.95328	2.3762x10 ⁻³	24.2755	1.8481	132.764
746	1.83x10 ⁻³	1019	0.98135	1.9947x10 ⁻³	24.2451	1.8504	111.311
716	1.68x10 ⁻³	989	1.0111	1.8312x10 ⁻³	24.2150	1.8527	102.0598
697	1.57x10 ⁻³	970	1.0309	1.7113x10 ⁻³	24.1961	1.8562	95.3

TABLE 13
Electrical Conductivity data of
Sample (8)

37 mole per cent V_2O_5

	V_2O_5	46.2328 gms.
	$Na_2B_4O_7$	0.7742 gms.
	B_2O_3	29.7948 gms.
Depth of melt	7.5 Div.	
C, Cell constant	1.18	
Density	ρ_8	
Molar Weight	111.1203	
Room temp volume corresponding to melt height (from chart)	40cc.	

Temp. °C	G_M Measured Conductivity ohm ⁻¹	Temp. T°K	$\frac{1}{T} \times 10^3$	K sp. conductivity ohm ⁻¹ cm ⁻¹	V_8 Volume of melt cc	ρ_8 Density of melt gms/cc	$\Lambda_M \times 10^4$ Molar Conductivity x 10 ⁴ ohm ⁻¹ mole ⁻¹ cm ²
859	1.59×10^{-2}	1132	0.88339	1.8762×10^{-2}	41.4603	1.8524	112.548
846	1.38×10^{-2}	1119	0.84745	1.6286×10^{-2}	41.4382	1.8534	97.63
821	1.14×10^{-2}	1094	0.91407	1.3452×10^{-2}	41.3960	1.8553	80.569
793	0.9×10^{-2}	1066	0.93809	1.0620×10^{-2}	41.3481	1.8574	63.535
771	0.69×10^{-2}	1044	0.95785	0.8142×10^{-2}	41.3107	1.8591	48.666
746	0.51×10^{-2}	1019	0.98135	0.6018×10^{-2}	42.2682	1.8610	35.9335
721	0.38×10^{-2}	996	1.0060	0.4686×10^{-2}	41.2260	1.8629	28.87
697	0.268×10^{-2}	970	1.0309	0.81626×10^{-2}	41.1849	1.8648	18.844

TABLE 14
Electrical Conductivity data of
Sample (9)

46.47 mole per cent V_2O_5

V_2O_5	46.2328 gms.
$Na_2B_4O_7$	0.5790 gms.
B_2O_3	19.8018 gms.
Depth of melt	7.1 Div.
C, Cell constant	1.17
Molar Weight	121.7567
Room temp volume corresponding to melt depth	37cc.

Temp °C	G_M Measured Conductivity ohm ⁻¹	Temp. T°K	$\frac{1}{T} \times 10^3$	K sp. conductivity ohm ⁻¹ cm ⁻¹	V_9 Volume of melt cc	ρ_9 Density of melt gms/cc	$\Lambda M \times 10^4$ Molar Conductivity $\times 10^4$ ohm ⁻¹ mole ⁻¹ cm ²
859	3.34×10^{-2}	1132	0.88339	3.9078×10^{-2}	38.3508	1.7370	278.921
851	3.12×10^{-2}	1124	0.88967	3.6504×10^{-2}	38.3382	1.7375	255.805
840	2.90×10^{-2}	1113	0.89847	3.393×10^{-2}	38.3209	1.7379	237.712
820	2.58×10^{-2}	1093	0.91491	3.0186×10^{-2}	38.2895	1.7397	211.2633
810	2.39×10^{-2}	1083	0.92336	2.7963×10^{-2}	38.2767	1.7406	195.6264
796	2.10×10^{-2}	1069	0.93545	2.457×10^{-2}	38.2517	1.7416	171.791
777	1.80×10^{-2}	1050	0.95238	2.1060×10^{-2}	38.2185	1.7630	147.114
746	1.33×10^{-2}	1019	0.98135	1.5561×10^{-2}	38.1731	1.7450	108.576
716	0.94×10^{-2}	989	1.0111	1.0998×10^{-2}	38.1259	1.7472	76.641
706	0.84×10^{-2}	979	1.0214	0.9828×10^{-2}	38.1100	1.7479	68.461
692	0.70×10^{-2}	965	1.0362	0.8190×10^{-2}	38.0878	1.7489	57.018

TABLE 15
Electrical Conductivity data of
Sample (10)

60.39 mole per cent V_2O_5

V_2O_5 46.2328 gms.
 $Na_2B_4O_7$ 0.3396 gms.
 B_2O_3 11.26489 gms.
 Depth of melt 6.6 Div.
 C, Cell constant 1.135
 Mol. Weight 137.3912
 Room temp volume corresponding to the melt height 33cc.

Temp. °C	G_M Measured Conductivity ohm ⁻¹ s	Temp. T°K	$\frac{1}{T} \times 10^3$	K sp. conductivity ohm ⁻¹ cm ⁻¹	V_{10} Volume of melt cc	ρ_{10} Density of melt gms/cc	$\Lambda_M \times 10^4$ Molar Conductivity x 10 ⁴ ohm ⁻¹ mole ⁻¹ cm ²
859	5.64x10 ⁻²	1132	0.88339	6.4016x10 ⁻²	34.2047	1.6909	520.135
855	5.44x10 ⁻²	1128	0.88652	6.1744x10 ⁻²	34.1992	1.6912	501.601
851	5.20x10 ⁻²	1124	0.88967	5.9020x10 ⁻²	34.1935	1.6915	479.387
839	4.70x10 ⁻²	1112	0.89928	5.3345x10 ⁻²	34.1768	1.6923	434.00
825	4.40x10 ⁻²	1098	0.91074	4.9940x10 ⁻²	34.1567	1.6933	405.204
810	3.92x10 ⁻²	1083	0.92336	4.4492x10 ⁻²	34.1369	1.6942	360.808
796	3.54x10 ⁻²	1069	0.93545	4.0179x10 ⁻²	34.1164	1.6953	325.62
772	2.92x10 ⁻²	1045	0.95693	3.3142x10 ⁻²	34.0888	1.6967	268.3691
752	2.56x10 ⁻²	1025	0.97560	2.9056x10 ⁻²	34.0550	1.6983	235.097
746	2.40x10 ⁻²	1019	0.98315	2.724x10 ⁻²	34.0403	1.6988	220.3047
724	1.96x10 ⁻²	1001	0.99900	2.246x10 ⁻²	34.0156	1.7003	181.486
696	1.48x10 ⁻²	969	1.0319	1.6798x10 ⁻²	33.9768	1.7023	135.575
692	1.41x10 ⁻²	965	1.0362	1.60035x10 ⁻²	33.9702	1.7026	129.136

TABLE 16
Electrical Conductivity data of
Sample (11)

73 mole per cent V_2O_5

V_2O_5 46.2328 gms.
 $Na_2B_4O_7$ 0.2112 gms.
 B_2O_3 6.4996 gms.

Depth of melt 6.3 Div.
C, Cell constant 1.10
Mol. Weight 151.554

Room temp volume corresponding to melt height 3lcc

Temp °C	G_M Measured Conductivity $ohm^{-1}s$	Temp. T°K	$\frac{1}{T^\circ K} \times 10^3$	K sp. conductivity $ohm^{-1}cm^{-1}$	V_{11} Volume of melt cc	ρ_{11} Density of melt gms/cc	$\Lambda_M \times 10^4$ Molar Conductivity $\times 10^4$ $ohm^{-1}mole^{-1}cm^2$
859	5.68×10^{-2}	1132	0.88339	6.248×10^{-2}	32.1317	1.6477	574.687
855	5.56×10^{-2}	1128	0.88652	6.1160×10^{-2}	32.1265	1.6479	562.478
848	5.44×10^{-2}	1121	0.89206	5.9860×10^{-2}	32.1174	1.6484	550.171
835	4.90×10^{-2}	1112	0.88928	5.390×10^{-2}	32.1005	1.6493	495.288
820	4.53×10^{-2}	1093	0.91491	4.983×10^{-2}	32.0804	1.6503	457.611
810	4.21×10^{-2}	1083	0.92336	4.631×10^{-2}	32.0680	1.6510	425.105
800	3.88×10^{-2}	1073	0.93196	4.268×10^{-2}	32.0540	1.6517	391.618
796	3.72×10^{-2}	1069	0.93545	4.092×10^{-2}	32.0687	1.6520	375.4
776	3.26×10^{-2}	1049	0.95328	3.564×10^{-2}	32.0230	1.6533	326.7
766	2.97×10^{-2}	1039	0.96246	3.2670×10^{-2}	32.0090	1.6540	299.352
756	2.71×10^{-2}	1029	0.97181	2.981×10^{-2}	31.9968	1.6546	273.047
746	2.45×10^{-2}	1019	0.98135	2.695×10^{-2}	31.9829	1.6554	246.731
716	1.78×10^{-2}	989	1.0111	1.958×10^{-2}	31.9633	1.6574	179.0416
696	1.60×10^{-2}	969	1.0319	1.54×10^{-2}	31.9176	1.6588	140.700

TABLE 17
Electrical Conductivity data of
Sample (12)

88 mole per cent V_2O_5

V_2O_5	46.2328 gms.
$Na_2B_4O_7$	0.0706 gms.
B_2O_3	2.4693 gms.
Depth of melt	6.0 Div.
C, Cell constant	1.080
Mol. Weight	169.402
Room temp. volume corresponding to melt height	29.5 cc.

Temp. °C	G_M Measured Conductivity ohm ⁻¹ s	Temp. T°K	$\frac{1}{T} \times 10^3$	sp. conductivity ohm ⁻¹ cm ⁻¹ GM x C	V_{12} Volume of melt cc	ρ_{12} Density of melt gms/cc	$\Lambda_M \times 10^4$ Molar Conductivity x 10 ⁴ ohm ⁻¹ mole ⁻¹ cm ²
850	3.88×10^{-2}	1123	0.89047	4.1904×10^{-2}	30.57	1.5954	442.315
839	3.66×10^{-2}	1112	0.89928	3.9528×10^{-2}	30.55	1.5965	416.947
835	3.58×10^{-2}	1108	0.90252	3.8664×10^{-2}	30.54	1.5970	407.711
820	3.26×10^{-2}	1093	0.91491	3.5208×10^{-2}	30.53	1.5975	371.148
815	3.14×10^{-2}	1088	0.91911	3.3912×10^{-2}	30.52	1.5980	357.372
804	2.88×10^{-2}	1077	0.92850	3.1104×10^{-2}	30.51	1.5985	327.682
796	2.70×10^{-2}	1069	0.93545	2.9160×10^{-2}	30.50	1.599	307.082
776	2.30×10^{-2}	1049	0.95328	2.4840×10^{-2}	30.47	1.6006	261.367
766	2.08×10^{-2}	1039	0.96426	2.2464×10^{-2}	30.46	1.6012	236.260
756	1.89×10^{-2}	1029	0.97181	2.0412×10^{-2}	30.45	1.6017	214.612
736	1.51×10^{-2}	1009	0.99109	1.6308×10^{-2}	30.42	1.6033	171.295
716	1.21×10^{-2}	989	1.0111	1.3068×10^{-2}	30.40	1.6044	137.164
696	0.90×10^{-2}	969	1.0319	0.9720×10^{-2}	30.37	1.6059	101.93
691	0.81×10^{-2}	964	1.0373	0.8478×10^{-2}	30.36	1.6064	91.703

TABLE 18
Electrical Conductivity data of
Sample (13)

95 mole per cent V_2O_5

V_2O_5 46.2328 gms.

$Na_2B_4O_7$ 0.0262 gms.

B_2O_3 0.9765 gms.

Depth of melt 5.80 Div.

C, Cell constant 1.04

Mol. Weight 176.264

Room temp. volume corresponding to melt depth 27.5cc.

Temp. °C	G_M Measured Conductivity ohm ⁻¹ s	Temp. T°K	$\frac{1}{T} \times 10^3$	K sp. conductivity ohm ⁻¹ cm ⁻¹	V_{13} Volume of melt cc	ρ_{13} Density of melt gms/cc	$\Lambda_M \times 10^4$ Molar Conductivity $\times 10^4$ ohm ⁻¹ mole ⁻¹ cm ²
859	6.02×10^{-2}	1132	0.88339	6.2608×10^{-2}	28.5040	1.6572	641.3172
854	5.94×10^{-2}	1127	0.88731	6.1776×10^{-2}	28.6983	1.6574	656.987
851	5.80×10^{-2}	1124	0.88967	6.0320×10^{-2}	28.4946	1.6577	641.386
839	5.42×10^{-2}	1112	0.89928	5.6368×10^{-2}	28.4807	1.6585	599.075
824	4.90×10^{-2}	1097	0.91157	5.0960×10^{-2}	28.4631	1.6595	541.273
815	4.66×10^{-2}	1088	0.91911	4.8256×10^{-2}	28.4525	1.6601	512.367
804	4.28×10^{-2}	1077	0.92850	4.4512×10^{-2}	28.4397	1.6609	472.387
796	4.06×10^{-2}	1069	0.93545	4.2226×10^{-2}	28.4303	1.6614	447.97
776	3.50×10^{-2}	1049	0.95328	3.640×10^{-2}	28.4075	1.6628	385.856
766	3.21×10^{-2}	1039	0.96266	3.338×10^{-2}	28.3955	1.6035	353.694
756	3.02×10^{-2}	1029	0.97181	3.1408×10^{-2}	28.3843	1.6641	332.679
743	2.76×10^{-2}	1016	0.98425	2.8706×10^{-2}	28.3682	1.6651	303.855
726	2.34×10^{-2}	999	1.0010	2.6336×10^{-2}	28.3485	1.6662	257.446
705	1.97×10^{-2}	978	1.0224	2.0488×10^{-2}	28.3241	1.6677	216.544
696	1.785×10^{-2}	969	1.0319	1.8564×10^{-2}	28.3150	1.6683	196.138

TABLE 19
Electrical Conductivity data of
Sample (14)

100 % V_2O_5
 V_2O_5 39.8636 gms.
 Depth of melt 5.2 Div.
 C, Cell constant 0.95
 Mol. Weight 181.88
 Room temp. volume corresponding to melt depth 23.5cc.

Temp. °C	G_M Measured Conductivity ohm^{-1}s	Temp. T°K	$\frac{1}{T} \times 10^3$	K sp. conductivity $\text{ohm}^{-1}\text{cm}^{-1}$ $G_M \times C$	V_{14} Volume of melt cc	ρ_{13} Density of melt gms/cc	$\Lambda_M \times 10^4$ Molar Conductivity $\times 10^4$ $\text{ohm}^{-1}\text{mole}^{-1}\text{cm}^2$
798	7.36×10^{-2}	1071	0.93370	6.992×10^{-2}	24.2971	1.6406	775.1463
782	6.003×10^{-2}	1055	0.94786	5.7028×10^{-2}	24.2800	1.6418	631.7610
762	5.50×10^{-2}	1035	0.96618	5.225×10^{-2}	24.2600	1.6632	578.3368
757	5.32×10^{-2}	1030	0.97087	5.056×10^{-2}	24.2567	1.6634	559.3413
751	5.18×10^{-2}	1024	0.97656	4.9210×10^{-2}	24.2501	1.6438	544.4893
744	4.72×10^{-2}	1017	0.98329	4.486×10^{-2}	24.2433	1.6443	495.9861
734	4.24×10^{-2}	1007	0.99304	4.028×10^{-2}	24.2332	1.6450	445.3572
728	3.98×10^{-2}	1001	0.999	3.7810×10^{-2}	24.2272	1.6454	417.946
720	3.74×10^{-2}	993	1.0070	3.5530×10^{-2}	24.2191	1.6459	392.2426
698	3.20×10^{-2}	971	1.0298	3.040×10^{-2}	24.1970	1.6495	335.6086
690	2.96×10^{-2}	963	1.0384	2.8120×10^{-2}	24.1885	1.6480	310.3438

TABLE 20
 $\frac{1}{T} \times 10^3$ vs. $\text{LOG}_{10} K$ DATA

FOR ACTIVATION ENERGY PLOTS

0 mole % V_{2O_5}		0.17 mole % V_{2O_5}		3 mole % V_{2O_5}	
$\frac{1}{T} \times 10^3$	$\text{log}_{10} K$	$\frac{1}{T} \times 10^3$	$\text{log}_{10} K$	$\frac{1}{T} \times 10^3$	$\text{log}_{10} K$
0.88339	4.6867	0.88339	4.9118	0.88339	4.9901
0.88967	4.6439	0.90009	4.8315	0.89525	4.9231
0.89525	4.6116	0.91240	4.7827	0.91996	4.8163
0.90961	4.5426	0.92850	4.7001	0.92850	4.7735
0.93196	4.4266	0.93545	4.6648	0.94339	4.6995
0.94696	4.3555	0.94251	4.6381	1.0010	4.3876
0.98716	4.1202	0.98716	4.3850	1.0204	4.2693
1.0277	5.7698	1.0111	4.2505	1.0309	4.1704
1.0741	5.5986	1.0277	4.1524	1.0570	4.0675
1.1013	5.4085			1.0775	5.9243
				1.1248	5.6104

20.0 mole % V_{2O_5}		13.6 mole % V_{2O_5}		25 mole % V_{2O_5}	
$\frac{1}{T} \times 10^3$	$\text{log}_{10} K$	$\frac{1}{T} \times 10^3$	$\text{log}_{10} K$	$\frac{1}{T} \times 10^3$	$\text{log}_{10} K$
0.88339	4.9864	0.88339	4.9760	0.88339	3.3062
0.89686	4.9265	0.89285	4.9703	0.89686	3.2427
0.91324	4.8652	0.91491	4.8285	0.91491	3.1843
0.92592	4.8032	0.93196	4.7605	0.93196	3.1242
0.93196	4.7842	0.95602	4.6545	0.95785	3.0348
0.95693	4.6699	0.98135	4.5220	0.98135	4.9445
0.97751	4.5628	1.0172	4.3351	1.10309	4.8195
0.99700	4.4716	1.0764	4.0084	1.0515	4.8048
1.1037	5.95626				

Table 20 (cont'd)

30 mole % V ₂ O ₅		37 mole % V ₂ O ₅		46.47 mole % V ₂ O ₅	
$\frac{1}{T^{\circ}K} \times 10^3$	$\log_{10} K$	$\frac{1}{T^{\circ}K} \times 10^3$	$\log_{10} K$	$\frac{1}{T^{\circ}K} \times 10^3$	$\log_{10} K$
0.88339	3.5611	0.88339	2.2732	0.88339	2.5920
0.88967	3.5465	0.89745	2.2116	0.89847	2.5306
0.89686	3.5259	0.91407	2.1287	0.91491	2.4798
0.90909	3.4967	0.93809	2.0261	0.93545	2.3904
0.92592	3.4490	0.95785	3.9107	0.95238	2.3234
0.95328	3.3758	0.98135	3.7795	0.98135	2.1920
0.98135	3.2999	1.0060	3.6517	1.0111	2.0411
1.0111	3.2627	1.0309	3.5000	1.0214	3.9925
1.0301	3.2332			1.0362	3.9133

60.37 mole % V ₂ O ₅		73 mole % V ₂ O ₅		88 mole % V ₂ O ₅	
$\frac{1}{T^{\circ}K} \times 10^3$	$\log_{10} K$	$\frac{1}{T^{\circ}K} \times 10^3$	$\log_{10} K$	$\frac{1}{T^{\circ}K} \times 10^3$	$\log_{10} K$
0.88339	2.8063	0.88339	2.7958	0.89047	2.6222
0.89928	2.7271	0.89206	2.7864	0.90252	2.5873
0.91074	2.6985	0.91491	2.6975	0.91491	2.5465
0.92336	2.6483	0.92336	2.6657	0.92850	2.4928
0.93545	2.6039	0.93545	2.6119	0.95328	2.3952
0.95693	2.2203	0.95328	2.5519	0.96426	2.3514
0.97560	2.4632	0.97181	2.4743	0.97181	2.3098
0.999	2.3514	0.99108	2.3838	0.99109	2.2124
1.0362	2.2061	1.0111	2.2918	1.0111	2.1160
		1.0319	2.1875	1.0319	3.9877
		1.0362	2.1653		

Table 20 (cont'd)

95 mole % V ₂ O ₅		100 mole % V ₂ O ₅	
$\frac{1}{T^{\circ}K} \times 10^3$	$\log_{10} K$	$\frac{1}{T^{\circ}K} \times 10^3$	$\log_{10} K$
0.88339	2.7966	0.88339	2.8446
0.89928	2.7510	0.94786	2.7561
0.91157	2.7072	0.96618	2.7181
0.92850	2.6485	0.97656	2.6921
0.95328	2.5611	0.99304	2.6051
0.97181	2.4969	1.0070	2.5506
0.99108	2.4269	1.0298	2.4829
1.0224	2.3114	1.0384	2.4490
1.0362	2.2447		

APPENDIX - II

ACTIVATION ENERGY PLOTS FOR SAMPLES 1 to 14
(FIGS 9 to 22)

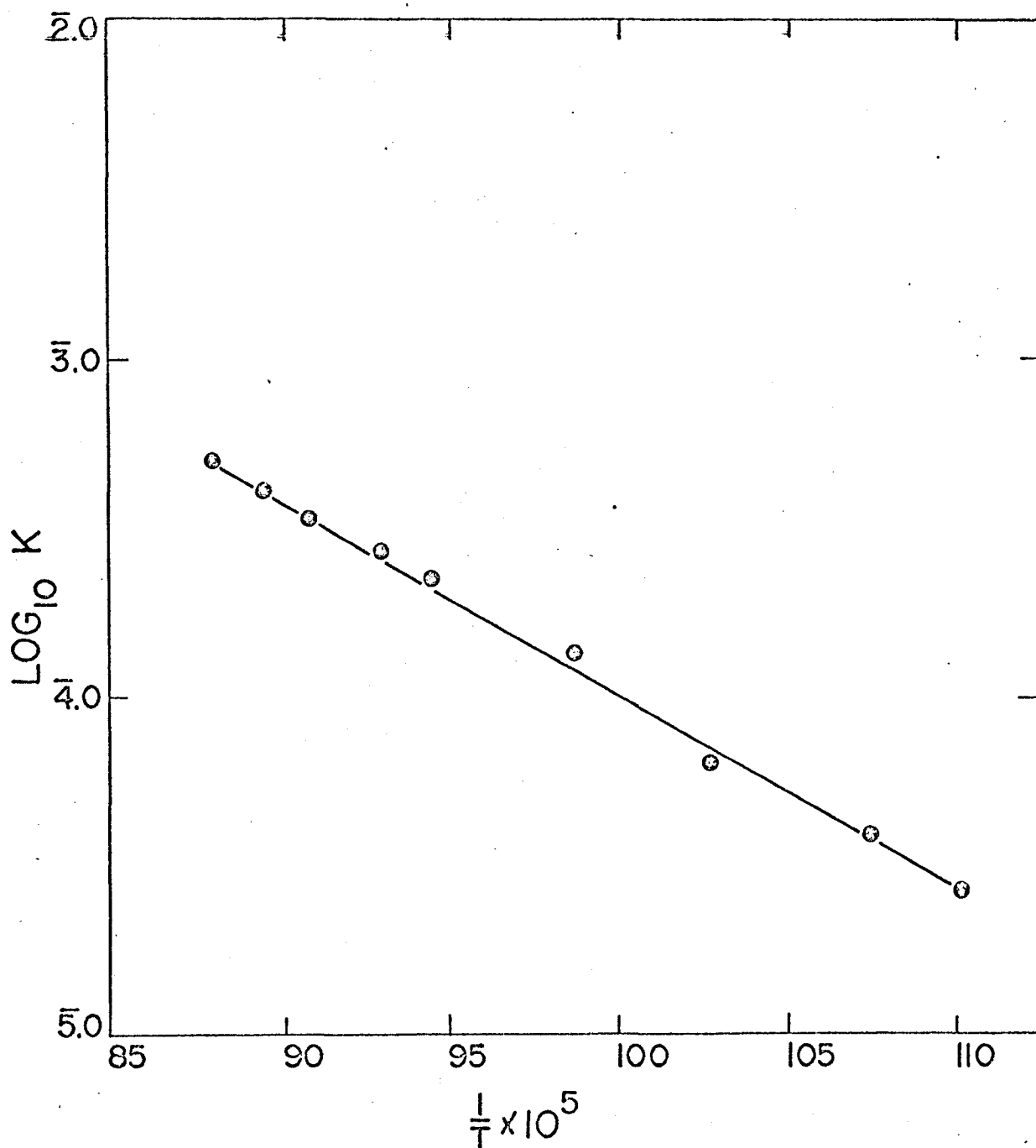


FIG. 9 $\text{LOG}_{10} K$ VS. $\frac{1}{T}$ CURVE FOR SAMPLE (1)
 (0 MOLE % V_2O_5)

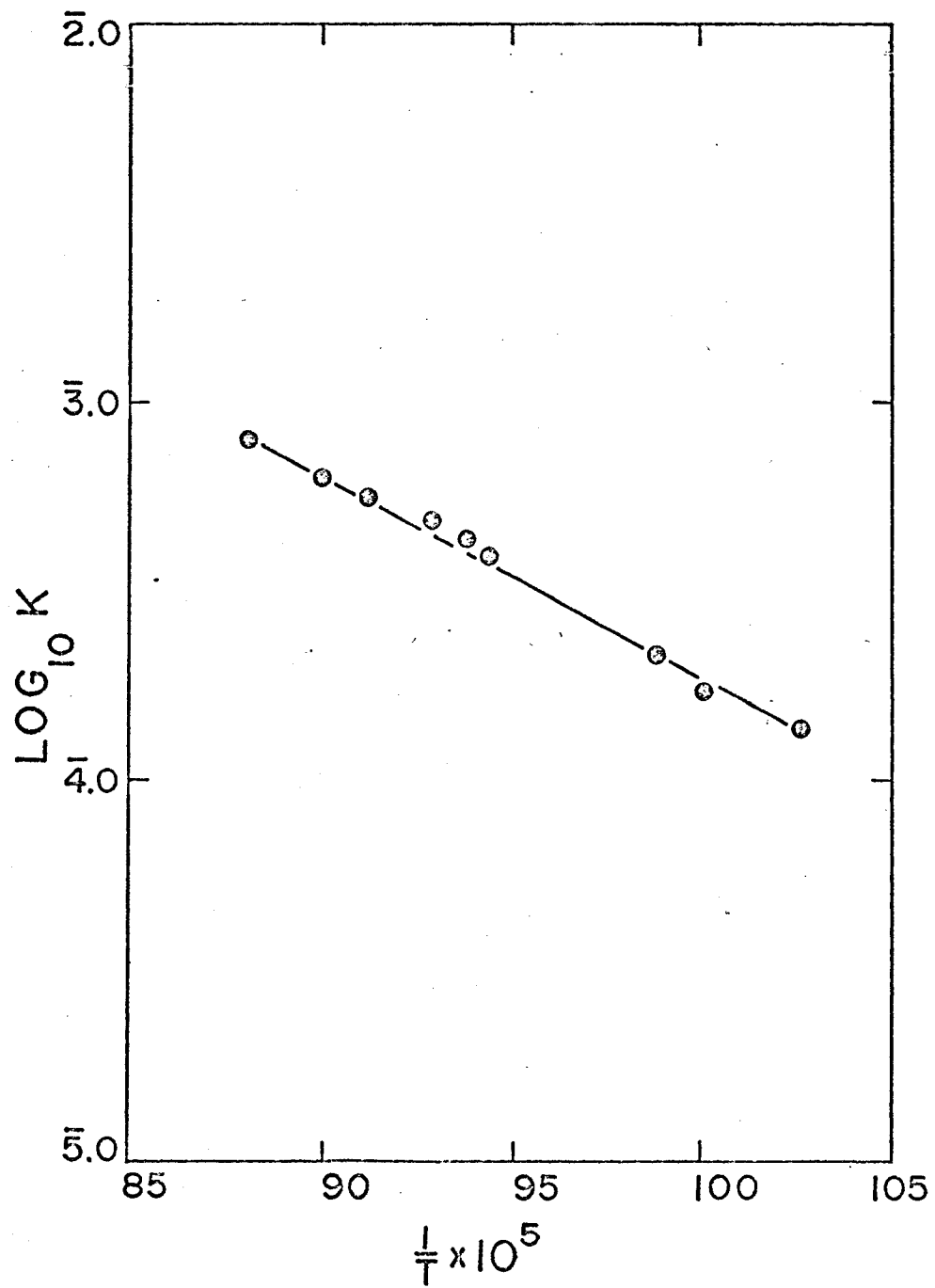


FIG.10 $\text{LOG}_{10} K$ VS. $\frac{1}{T}$ CURVE FOR SAMPLE (2)
 (0.17 MOLE % V_2O_5)

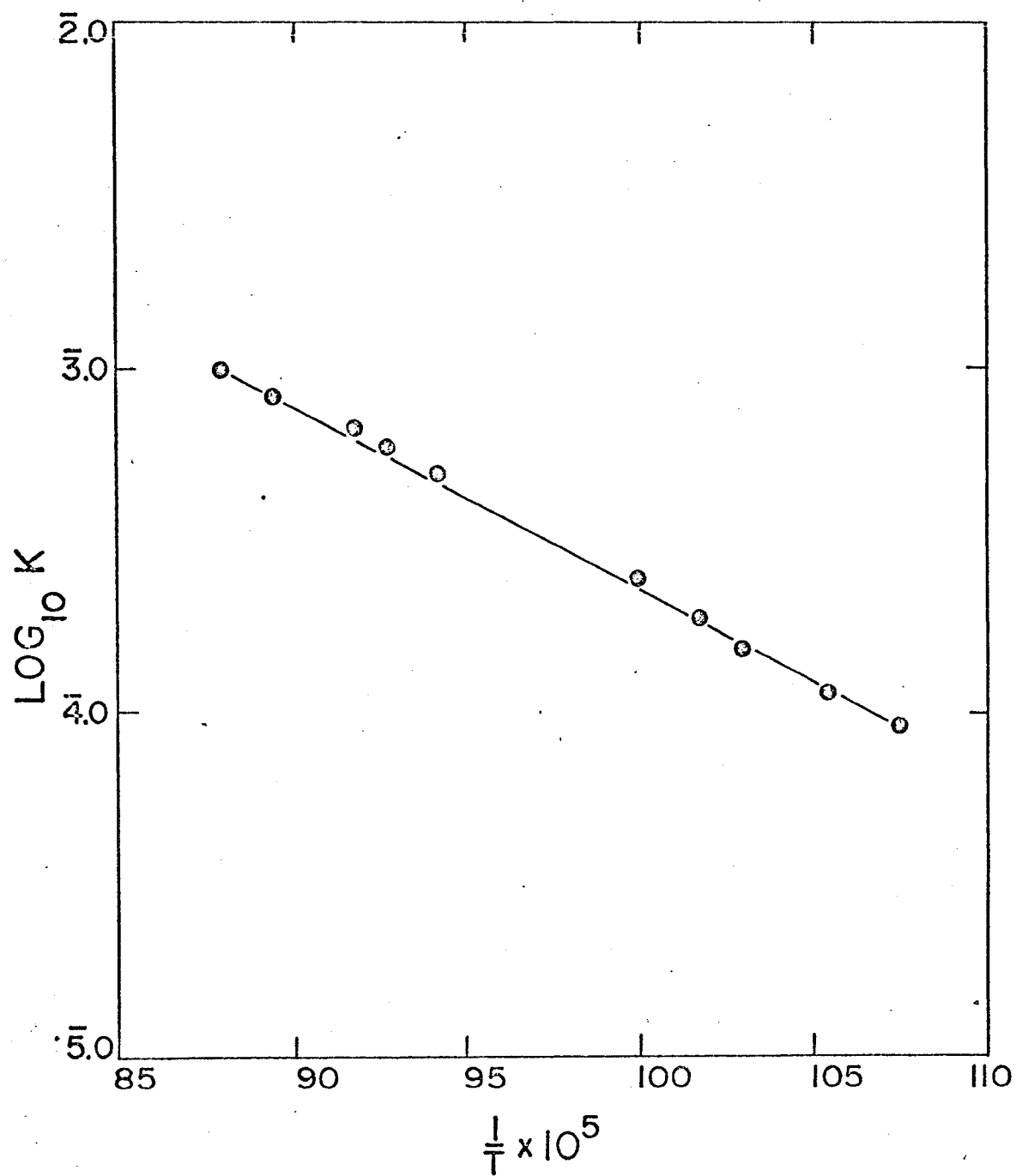


FIG. 11 $\text{LOG}_{10} K$ VS. $\frac{1}{T}$ CURVE FOR SAMPLE (3)
(3 MOLE % V_2O_5)

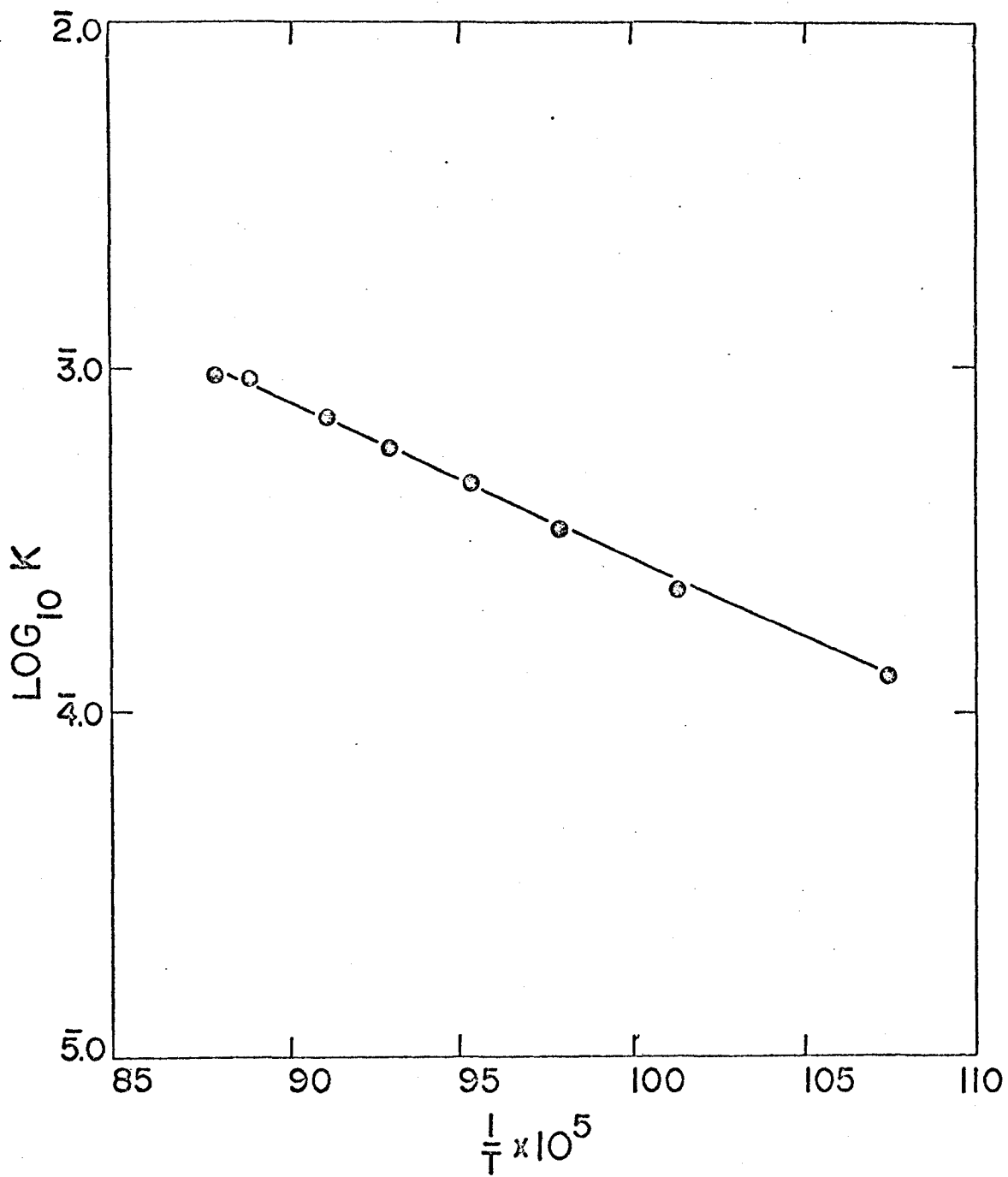


FIG. 12 $\text{LOG}_{10} K$ VS. $\frac{1}{T}$ CURVE FOR SAMPLE (4)
 (13.6 MOLE % V_2O_5)

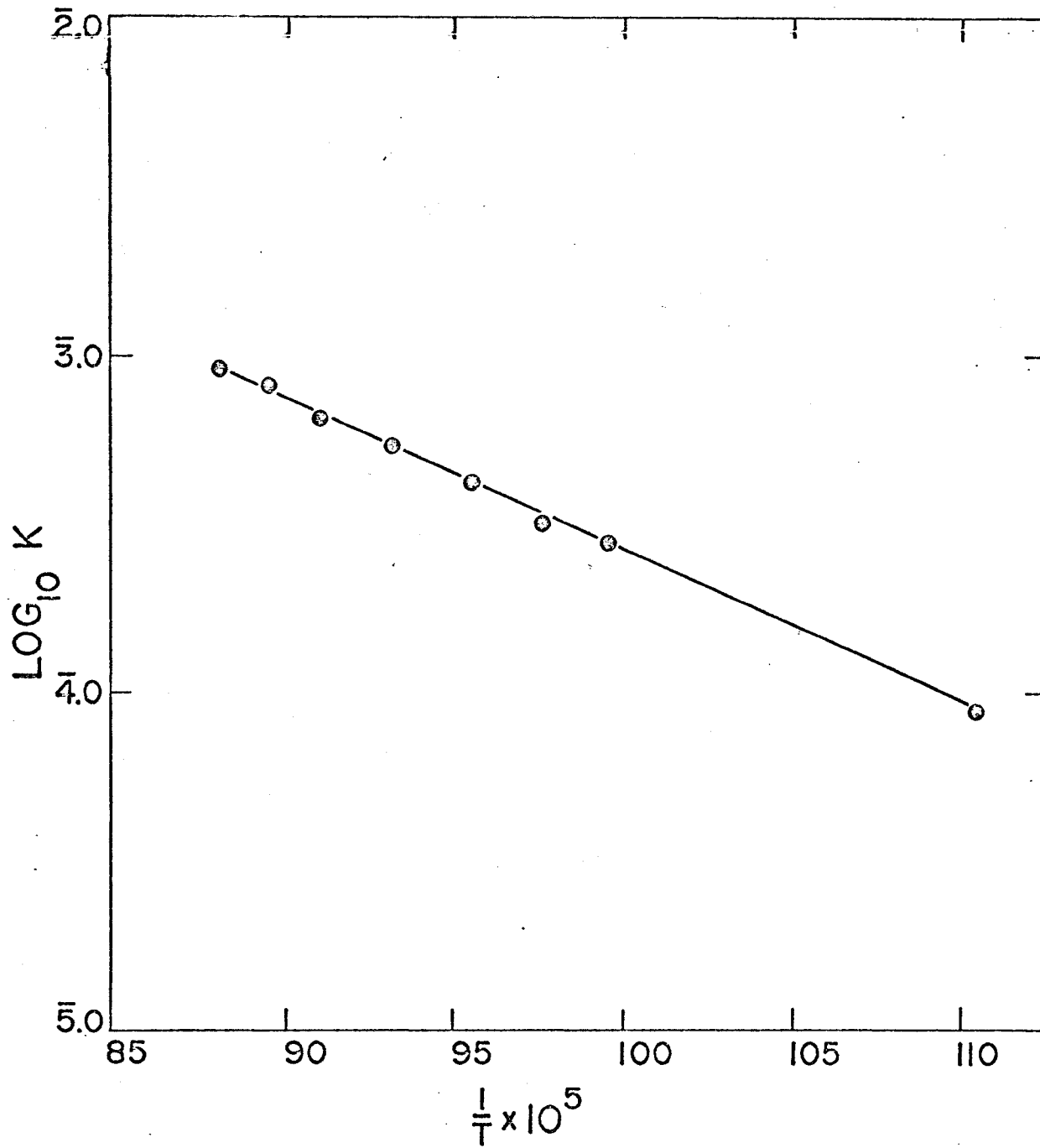


FIG. 13 $\text{LOG}_{10} K$ VS. $\frac{1}{T}$ CURVE FOR SAMPLE (5)
(20 MOLE % V_2O_5)

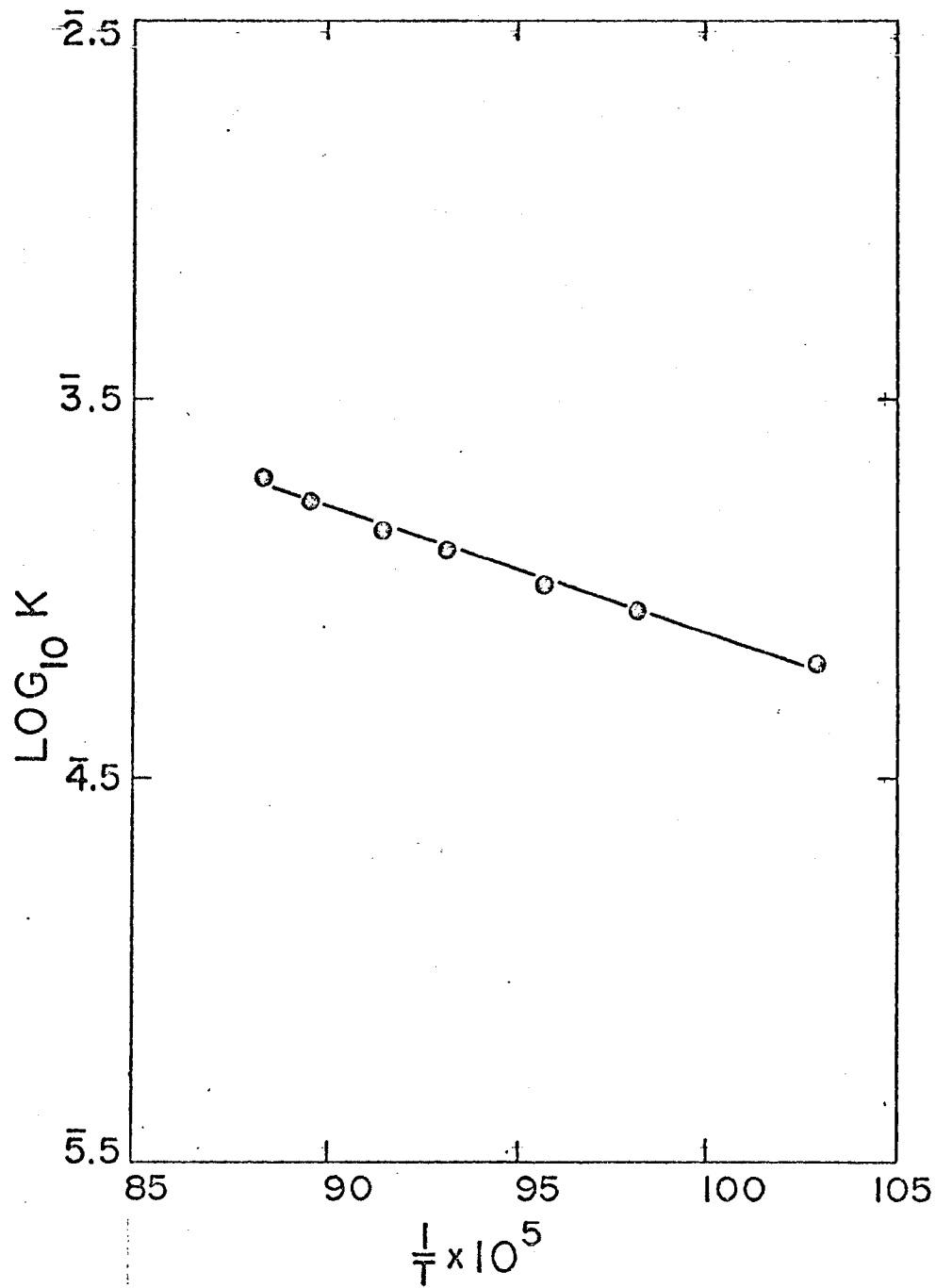


FIG. 14 $\text{LOG}_{10} K$ VS. $\frac{1}{T}$ CURVE FOR SAMPLE (6)
(25 MOLE % V_2O_5)

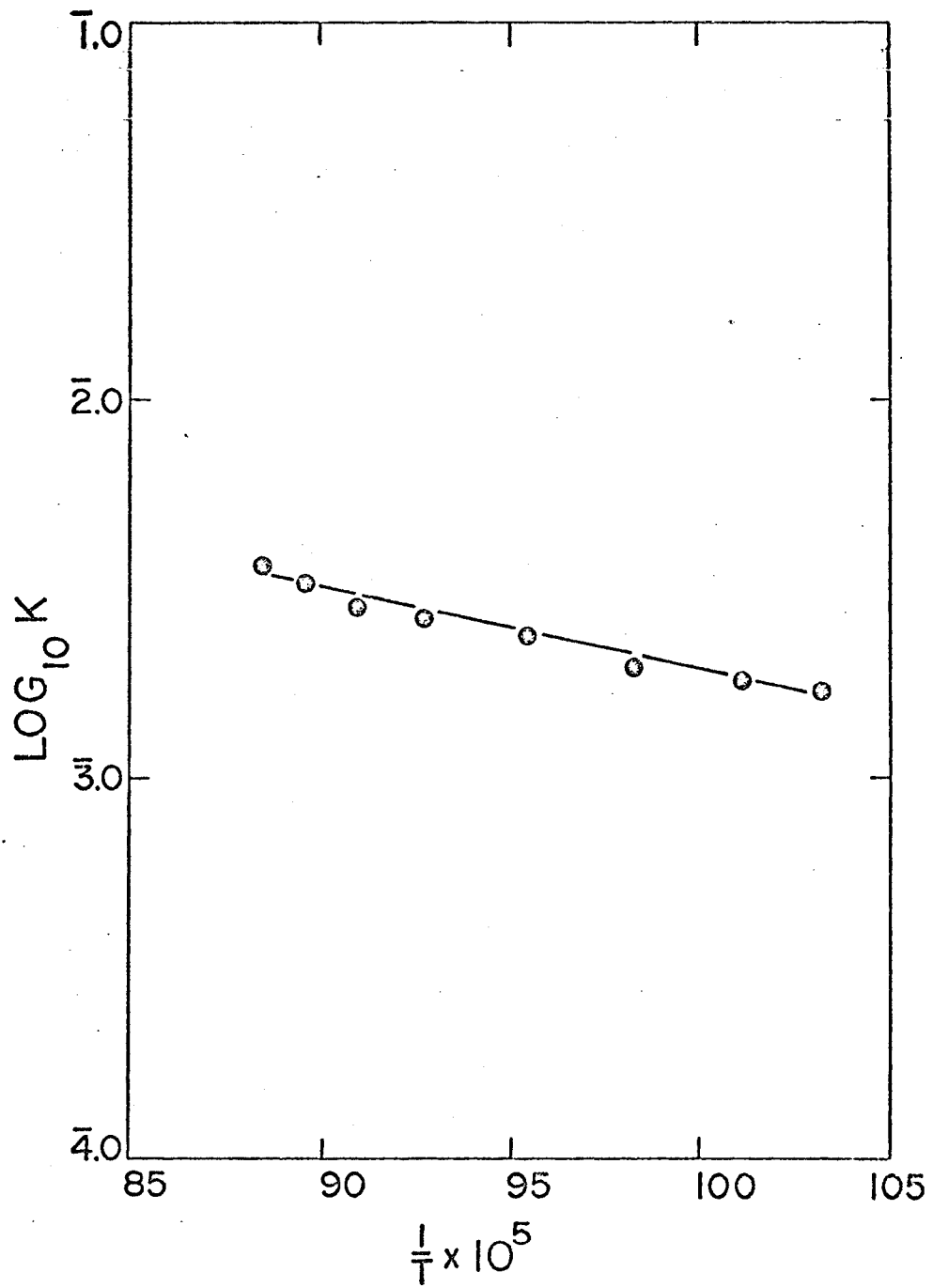


FIG. 15 $\text{LOG}_{10} K$ VS. $\frac{1}{T}$ CURVE FOR SAMPLE (7)
 (30 MOLE % V_2O_5)

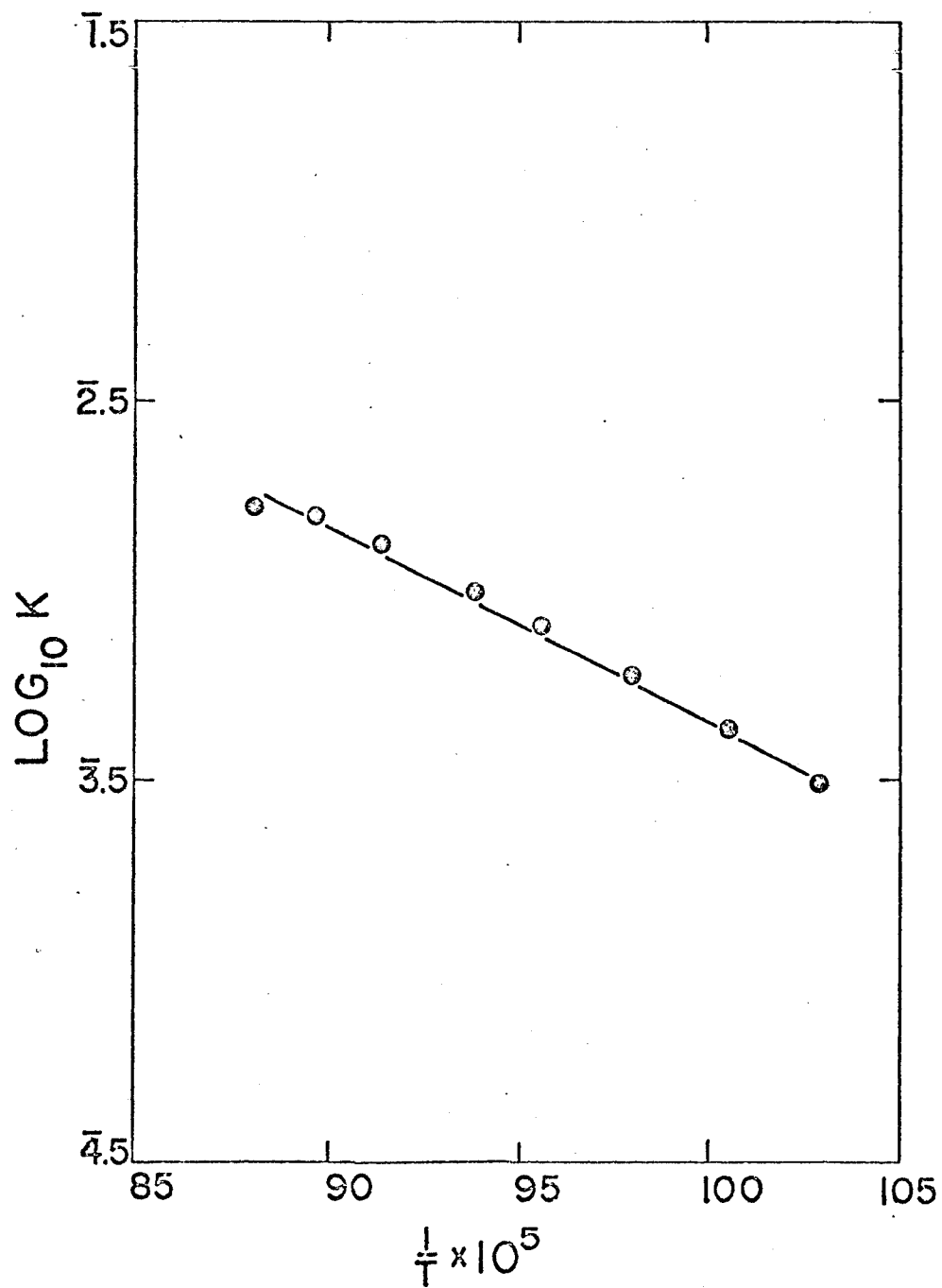


FIG. 16 $\text{LOG}_{10} K$ VS. $\frac{1}{T}$ CURVE FOR SAMPLE (8)
(37 MOLE % V_2O_5)

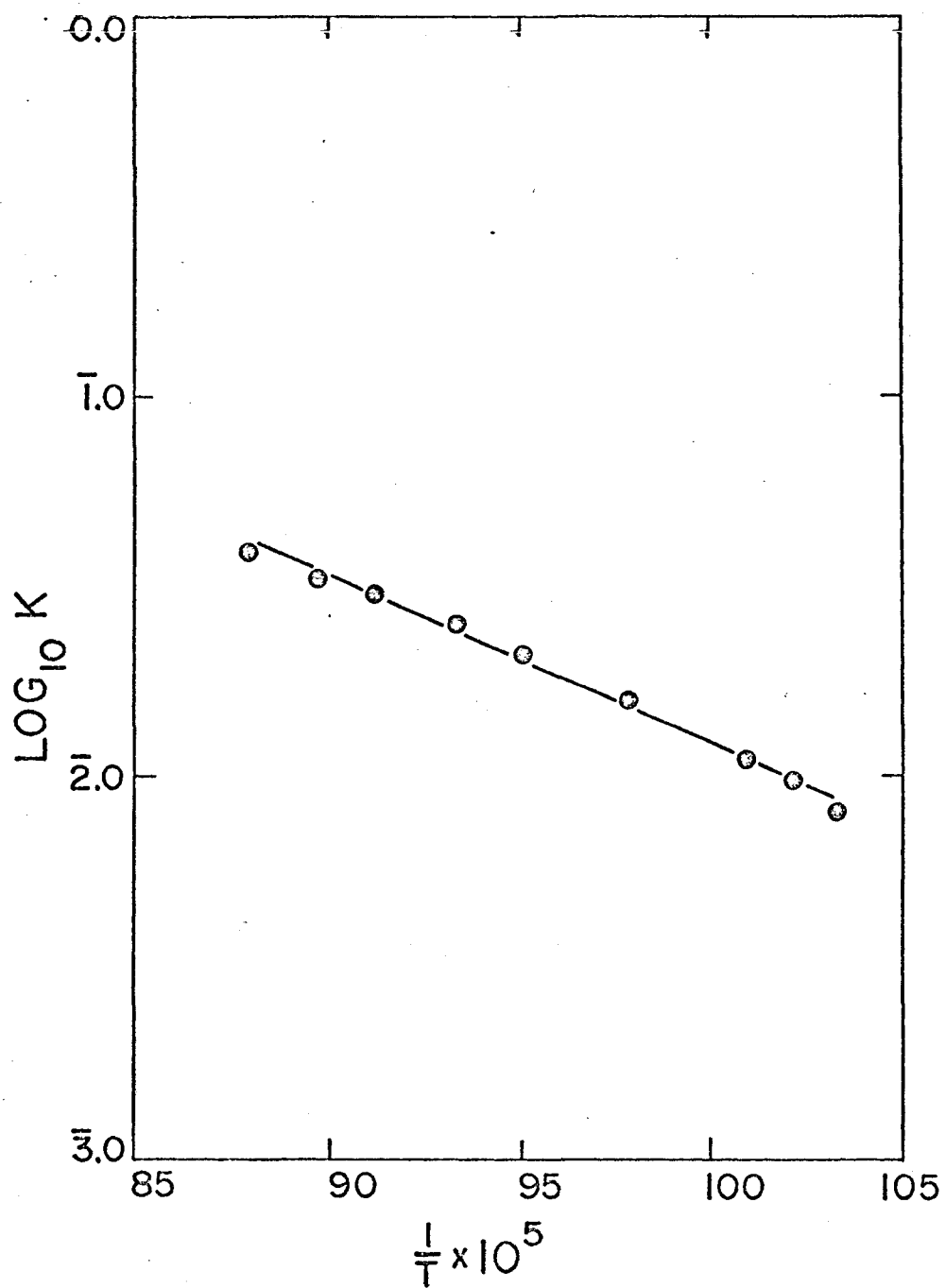


FIG. 17 $\text{LOG}_{10} K$ VS. $\frac{1}{T}$ CURVE FOR SAMPLE (9)
 (46.47 MOLE % V_2O_5)

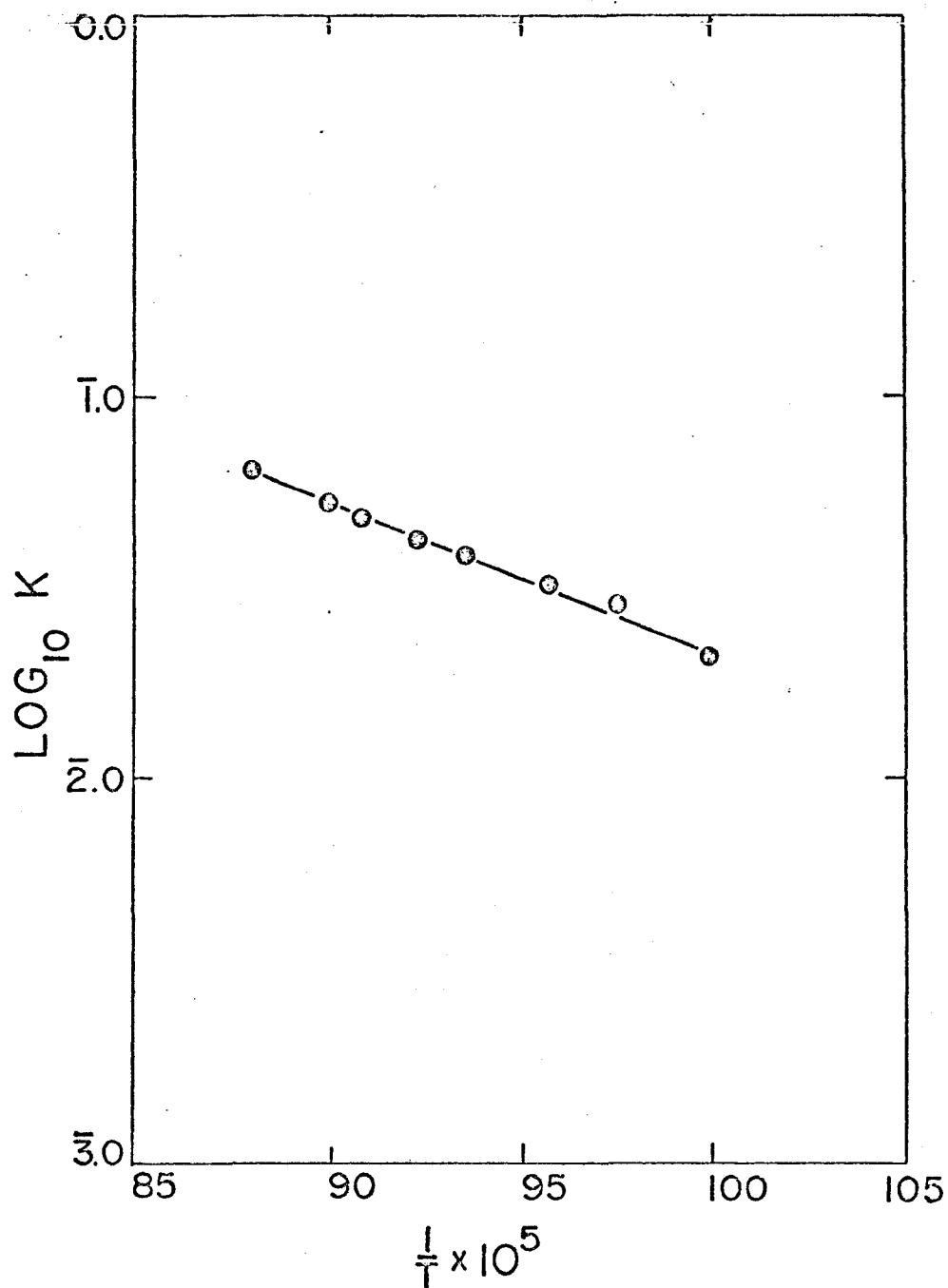


FIG. 18 $\text{LOG}_{10} K$ VS. $\frac{1}{T}$ CURVE FOR SAMPLE (10)
 (60.39 MOLE % V_2O_5)

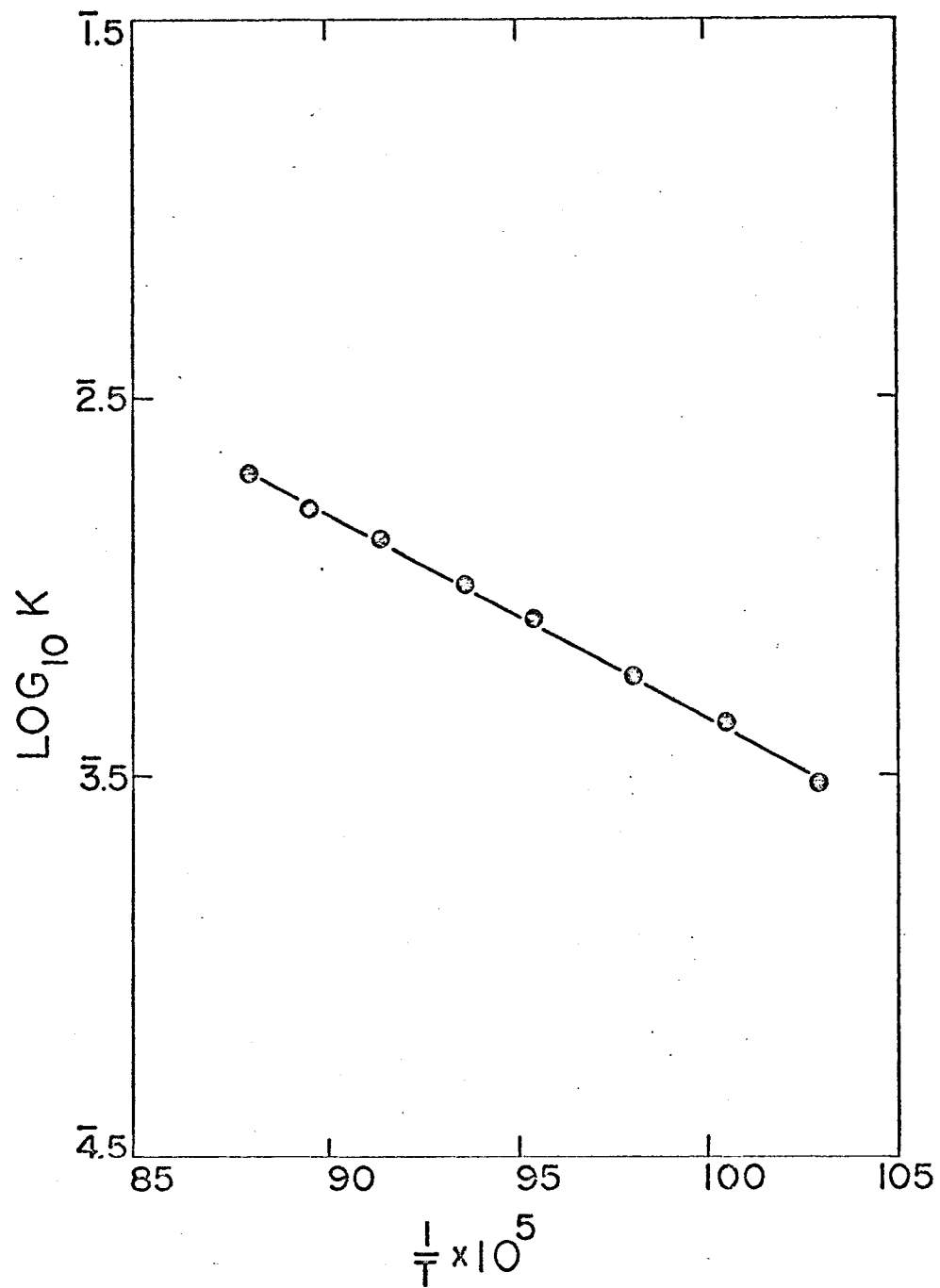


FIG. 19 $\text{LOG}_{10} K$ VS. $\frac{1}{T}$ CURVE FOR SAMPLE (11)
 (73 MOLE % V_2O_5)

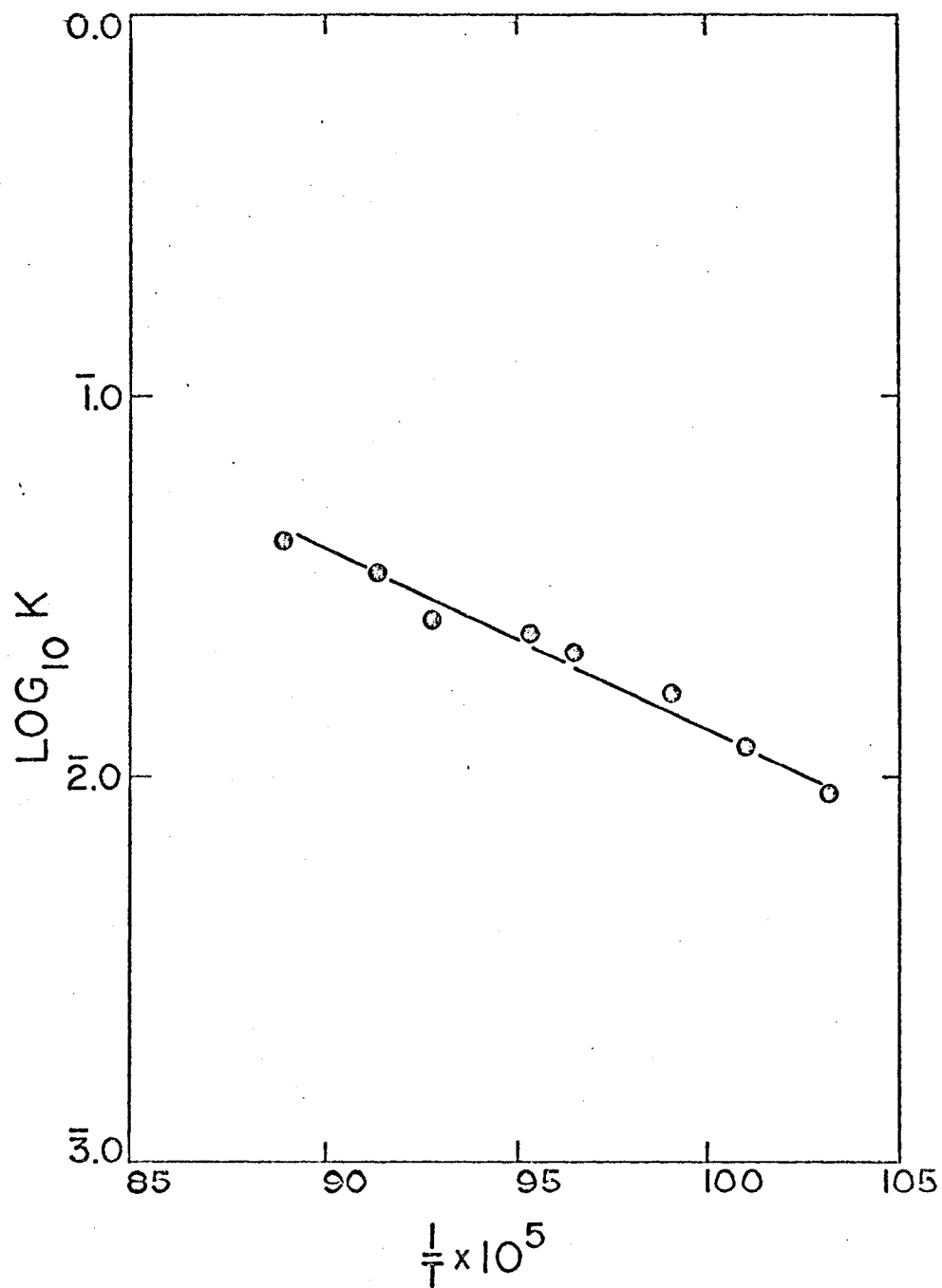


FIG. 20 $\text{LOG}_{10} K$ VS. $\frac{1}{T}$ CURVE FOR SAMPLE (12)
 (88 MOLE % V_2O_5)

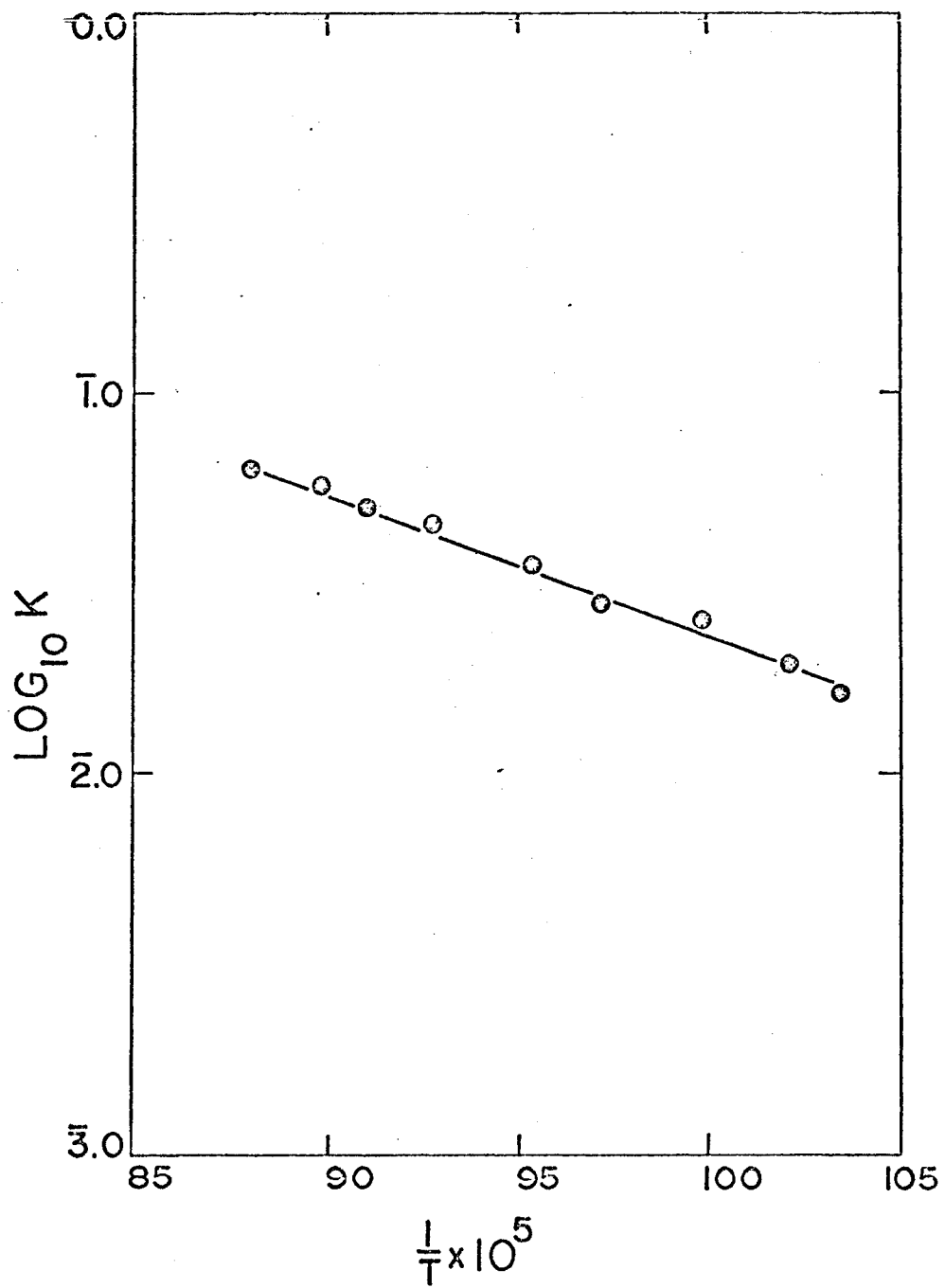


FIG. 21 $\text{LOG}_{10} K$ VS. $\frac{1}{T}$ CURVE FOR SAMPLE (13)
(95 MOLE % V_2O_5)

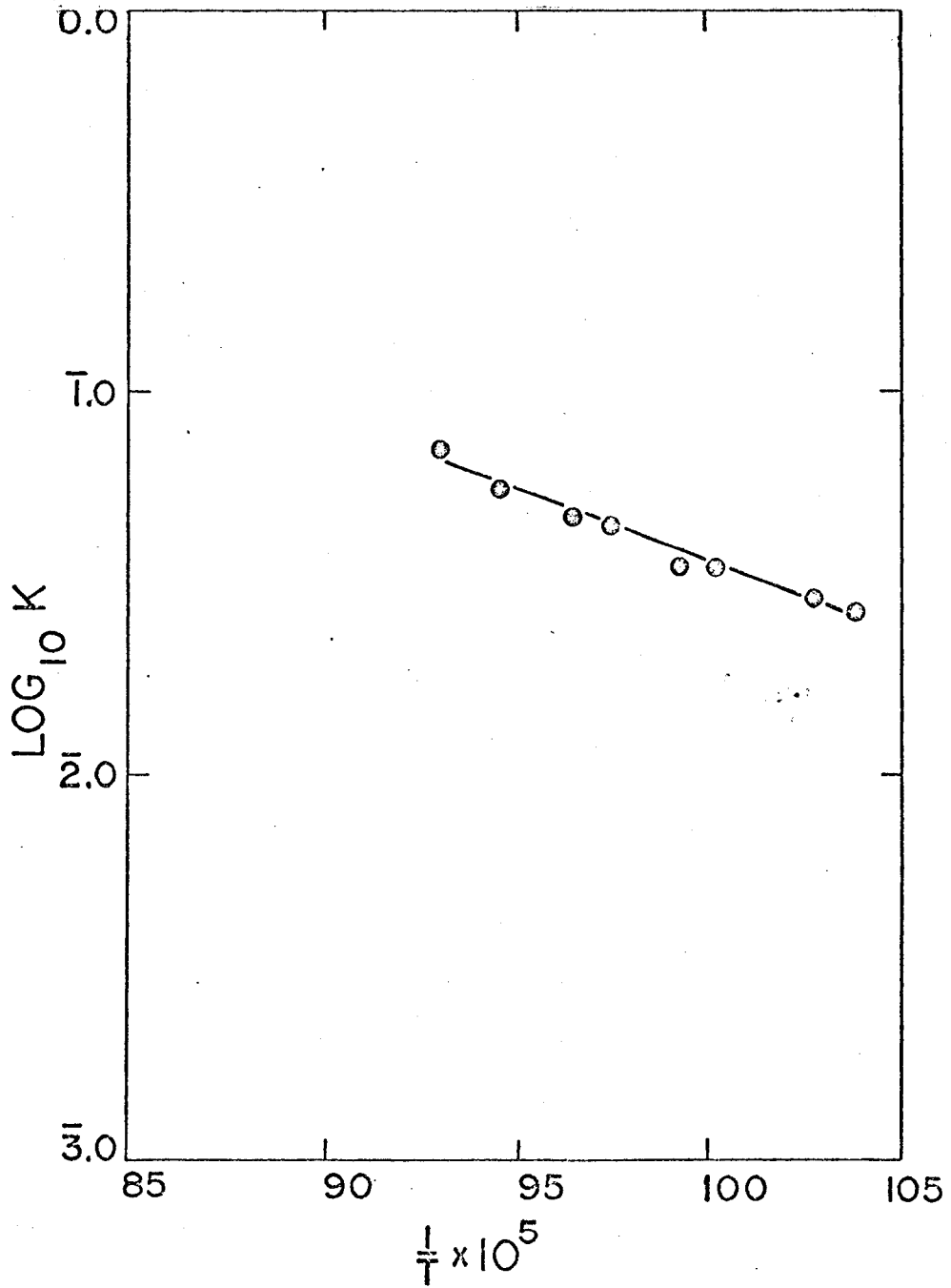


FIG. 22 $\text{LOG}_{10} K$ VS. $\frac{1}{T}$ CURVE FOR SAMPLE (14)
(Pure V_2O_5)

APPENDIX - III

NOMENCLATURE

Temperature °K	T
Specific Conductivity,) ohm ⁻¹ cm ⁻¹)	K
Cell constant, cm ⁻¹	C
Number of charges/ion	Z
Ionic radius	r
Depth of melt, cms	H
Molar weight, M = (1 - x) 69.653 + x . 181.88 where x = mole fraction of V ₂ O ₅	
Density of melt, gms/cc where i is the sample number	ρ _i
Volume of melt, cc where i is the sample number	V _i
Measured conductance, mhos	G _M
Molar conductivity, ohm ⁻¹ cm ⁻¹ cm ²	Λ _M = $\frac{K \cdot M}{\rho_i}$

VITA AUCTORIS

- 1937 Born in Tritala, Kerala, India.
- 1959 Graduated from the University of Kerala, India, with the degree of B.Sc (Chemistry main, Physics and Mathematics minor).
- 1961 Graduated from the University of Indian Institute of Science, Bangalore, India, with the degree of B.E (Met).
- 1968 Accepted to the Graduate School of the University of Windsor as a candidate for the degree of M.A.Sc in Engineering Materials.